I give permission for public access to my thesis and for copying to be done at the discretion of the archives' librarian and/or the College library.

_____ _____

Signature Date

****

THE ROLE OF REGENERATING ISLET-DERIVED 1 (REG1) PROTEIN IN THE MAIDS MODEL

by

Ifeoluwa Opeyemi Abeni Olokode

A Paper Presented to the
Faculty of Mount Holyoke College in
Partial Fulfillment of the Requirements for
the Degree of Bachelors of Arts with
Honor

Department of Biological Sciences
South Hadley, MA 01075

May 2013

****

This paper was prepared

under the direction of

Professor Sharon Stranford

for eight credits.

****

This thesis is dedicated to God for seeing me throughout my time at Mount Holyoke and for freely giving me his love that never fails, never gives up, never runs out on me.

ACKNOWLEDGEMENTS

To the main reason why this thesis is standing and printed: Prof. Sharon Stranford. I accidentally stumbled upon your lab meeting and you welcomed me with open arms. I am not sure if thank you will suffice for your continuous supportive attitude and your genuine belief in me even when I was too tired to believe in myself. It might not suffice but I will say it anyway: Thank you for everything!

To Prof. Janice Gifford: Thank you for the many hours you spent looking at my heaps of data and helping me come up with the best ways to analyze it.

To my fellow Stranford Lab mates: Stephanie Gu for being my partner in crime and for (mostly) always wanting to accompany me into lab at odd hours of the night. To Zaidat, Mtise, Beza, Erin and Chenyue, thank you for being wonderful, enthusiastic lab mates. Without your help, doing this research would have definitely taken longer than a year. Special thanks Stephanie Roses for patiently showing me how to navigate around a lab when I was clueless.

During this work, I was fortunate enough to collaborate with people who have facilitated breakthroughs and I especially want to extend my warmest thanks to Caroline Weber for her assistance.

To my academic advisor, Prof. Craig Woodard: Thank you for your continuous encouragement and support.

To my thesis committee members: Prof. Rachel Fink and Prof. Shelia Browne, thank you for agreeing to be a part of the last chapter in my Mount Holyoke career.

To Macy and Abena: Thank you for paving the way. You guys rock!

To my friends: The G8, thank you for a wonderful senior year! I am blessed to know you and call you all friends. Rukayat Taiwo, thank you for this beautiful thesis template and for calming me down when I was bouncing off the wall with anxiety. Thank you, Erica Monrose, for your superb editing skills. I am so grateful!

Despite the geographical distance, my family has always been behind me. Thank you, Mum and Dad for loving me, praying for me and putting up with my disappearances during this period. I love you!

TABLE OF CONTENTS

LIST OF FIGURES

LIST OF TABLES

ABSTRACT

Murine acquired immune deficiency syndrome (MAIDS) caused by the LP-BM5 isolate of Murine Leukemia Virus (MuLV), is an animal model used to study HIV-induced AIDS. After infection with the virus, the MAIDS susceptible C57BL/6 strain becomes immunocompromised and develops symptoms similar to that of humans infected with HIV-1. Conversely, MAIDS resistant BALB/c animals overcome their MuLV infection and gain adaptive immunity against subsequent challenge. Although it has been established that T cells and the genes found in the major histocompatibility complex (MHC) play a vital role in the outcome of MuLV infection, recent studies have identified genes outside the MHC that also play a role in MAIDS susceptibility One resistance-associated gene, regenerating islet-derived 1 (Reg1), was found to be highly expressed in the lymph node and spleen of recently infected BALB/c mice, with much lower expression seen in the susceptible BL/6 strain. The aim of this study was to design an enzyme-linked immunosorbent assay (ELISA) that could be used to identify the murine Reg1 protein and quantify its concentration in mouse tissue samples. Results with this assay show no significant difference the Reg1 expression in spleen and peripheral lymph node tissues between BALB/c and BL/6 mice at both naïve and infected states. However, when examined, the mesenteric lymph node showed a statistically significant difference in the expression of Reg1 between BALB/c and BL/6.

INTRODUCTION

Arguably the worst pandemic to affect humans, the Acquired Immune Deficiency Syndrome (AIDS) is a disease caused by the Human Immunodeficiency Virus (HIV) that attacks the human immune system and leads to its eventual collapse (Weiss, 1993). Since its discovery in the early 1980's (Levy, 1993), HIV infection was identified as the cause of approximately 30 million deaths by 2009 (UNAIDS, 2009). By 2010, there were as many as 34 million people living with the infection including the 2.7 million new infections recorded that same year (UNAIDS, 2011).

It has been established that the prevalence of HIV/AIDS is dependent on various factors such as education (Aggleton *et al.*, 2011; Baker *et al.*, 2011) and socioeconomic status (Perry, 1998) and this is illustrated by the geographical distribution of the disease. Sub-Saharan Africa is the region most affected by this disease, with 20 of its developing nations topping the list of the most HIV prevalent countries (UNAIDS, 2013). Unlike their more developed counterparts such as Germany with 0.1 percent HIV prevalence in people between the ages 15 – 49, and the United Kingdom with 0.3 percent HIV prevalence, developing countries like Swaziland and Botswana have 26 percent and 24 percent HIV prevalence respectively (UNAIDS, 2013). This disproportionate distribution of

the disease can be attributed to various factors including poverty, limited access to health care and anti-retroviral dugs, illiteracy and untreated sexually transmitted diseases (STDs) (Corbett *et al.*, 2002). Naturally, the regions with the most HIV prevalence have the highest numbers of HIV/AIDS related deaths. Most of these HIV related deaths are caused by concurrently occurring infectious diseases such as malaria and tuberculosis, diseases also mostly widespread in these areas (Corbett *et al.*, 2002).

Although recent advancements in science, such as the development of anti-retroviral drugs, have led to a reduction in the rates of HIV/AIDS related deaths (UNAIDS 2011), the statistics above indicate that the AIDS pandemic is far from over. In order to uncover how HIV evades the body's defenses, the body's fully functioning immune system must first be understood.

The Immune System

The mammalian body has several barriers in place to prevent the invasion of disease causing pathogens. Of these barriers, the skin, made of keratinized cells protecting a layer of epithelium, is the largest one. In addition to serving as a protective outer covering to the rest of the body, the skin also secretes substances that inhibit bacterial growth (Parham, 2009). The epithelial layer *sans* the

keratinized cells continues on to line the gastrointestinal, respiratory and urinary tracts, parts of the body that come in closest contact to the external environment after the skin. In place of keratinized cells, the epithelial layers lining these tracts are covered in glycoprotein, proteoglycan and enzyme containing mucus, which they secrete to prevent damage and limit infection. Coupled with the mucus secreting epithelial layer in the respiratory tract are epithelial cells equipped with beating cilia. These cilia continuously clear out the mucus secreted and with it, any foreign material, including pathogens, which may have been inhaled. The acidic environments of the stomach, vagina and skin also hinder the proliferation of microorganisms (Parham, 2009).

The epithelial layers of the body are in close contact with blood vessels; therefore if pathogens happen to make their way past these barriers, effector cells in the blood immediately activate the body's defense system, called the immune system.

The Innate Immune System

Once the barrier between the body and the external environment is broken and pathogens are introduced into the body, the innate immune system kicks in. The innate immune system is comprised of effector cells such as

monocytes, macrophages, dendritic cells, natural killer (NK) cells, mast cells and granulocytes (eosinophils, basophils and neutrophils). These cells and anti-microbial proteins, some of which already reside in the damaged tissue, are the first responders at the site of infection (Parham, 2009). These cells and proteins recognize the pathogens as invaders and start a series of reactions that often lead to the elimination or neutralization of the intruder. However, for the innate immune system to be effective, it first has to be able to distinguish intruder from self (Parham, 2009). To aid them in recognizing invading microbial pathogens, effector cells of the innate immune system possess germline-encoded molecular structures called pattern-recognition receptors (PRRs) that can be found both intracellularly and on the surface of their membranes (Parham, 2009; Beutler, 2004). These PRRs bind to pathogen-associated molecular patterns (PAMPs), unique molecular structures specific to different types of pathogens. Because these PAMPs are essential for the survival of the microorganism, they are rarely altered and thus make the pathogen easily recognizable by effector cells (Akira *et al.*, 2006). Examples of PAMPs are bacterial cell wall components made up of carbohydrates, lipids and lipopolysaccharide (LPS), cell structures such as flagellin, and viral structures such as double stranded RNA (Parham, 2009). The corresponding PPRs on cells of the innate immune response include lectins and toll-like receptors, which recognize pathogens at the cell membrane or lysosome membranes, and nucleotide-binding oligomerization domain - ligand recognition

receptor (NOD-LRR) and retinoic-acid-inducible protein I (RIG-I), which detect pathogens that have invaded the cell's cytosol (Akira *et al.*, 2006).

Toll-like receptors (TLRs) are a family of receptors responsible for recognizing a wide range of microbial structures. Each TLR is specific for recognizing a set of PAMPs. For example, TLR4, which can be found on macrophages and dendritic cells, recognizes lipopolysaccharide, fibronectin and heat-shock proteins (Akira *et al.*, 2006). The recognition of pathogen by a macrophage's toll-like receptor stimulates the macrophage to produce and release cytokines, small proteins that influence other cells' behavior by binding to receptors on their surfaces. Some of these cytokines include pro-inflammatory cytokines such as IL-1 and IL-6, which trigger the vasodilation of blood vessels, facilitating the entrance of more effector cells into the infected area; CXCL8, which actively recruits and directs neutrophils to the site of infection; and TNF-α, which triggers blood clotting, preventing pathogens from entering the blood stream and spreading infection throughout the body (Parham, 2009).

Should the invading pathogen be a bacterium or extra cellular virus particle, the actions of the effector cells are supplemented by soluble plasma proteins made by the liver called complement (Parham, 2009). Complement proteins coat pathogens, tagging them for destruction and making them more easily phagocytosized by effector cells such as macrophages. In some cases,

complement proteins organize the formation of protein complexes that damage the pathogen's membrane, and fragments of these proteins break off to recruit more immune cells to the site of infection (Parham, 2009).

The Adaptive Immune System

Sometimes, the immediate and non-specific actions of the innate immune system are not sufficient to conquer infection and a more targeted immune response is needed. This is where the slower but more specific adaptive immune response takes over. Dendritic cells, effector cells that are part of innate immunity, also play an important role in initiation of the adaptive immune system (Parham, 2009). During an infection, dendritic cells carry pathogens from the site of infection via lymphatic vessels into the draining lymph node (or the closest secondary lymphoid organ) where they trigger the adaptive immune response (Figure 1).

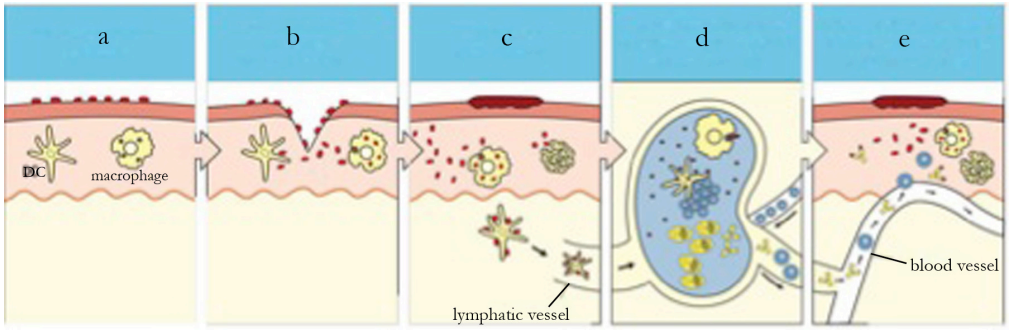

Figure 1. Dendritic cells carry invading pathogens from site of infection to draining lymph node where adaptive immune response is activated.

(a) Skin acts as a barrier preventing pathogens from gaining entry into the body. (b) Once the skin's barrier is broken, pathogens can access the connective tissue beneath the epithelium and here they encounter the innate immunity's defenses. (c) Dendritic cells, one of the innate immunity's defenses and also part of the adaptive immune response, carry some of the invading pathogens and their components via the lymph to the draining lymph node. (d) In the draining lymph node, pathogen-carrying dendritic cells activate the adaptive immune response by stimulating T cells (small blue cells). (e) The stimulation of T cells by dendritic cells leads to the production of antibodies and effector T cells (larger blue cells), the key players in the adaptive immune response that travel from the lymph node to the infected region via lymph and blood. Image adapted from Parham, 2009.

The adaptive immune response is activated when these pathogen carrying effector cells encounter B cells and T cells, the main effector cells of the adaptive immune system. Although slower than the innate immune system in responding during the first exposure to a particular pathogen (primary infection), upon subsequent (secondary) infection with the same pathogen, the more complex adaptive immune system responds faster than the innate response (Parham, 2009). The adaptive immune system's response to subsequent infection is often times so intense and precise that common symptoms of infection such as fever and inflammation are often undetectable by the host (Parham, 2009). Figure 2 illustrates the importance of having both innate and adaptive immune responses. B Cells and T Cells, the main effector cells of the adaptive immune system which arise from a common lymphoid progenitor cell, overcome infections through processes called the humoral immunity and cell-mediated immunity, respectively.

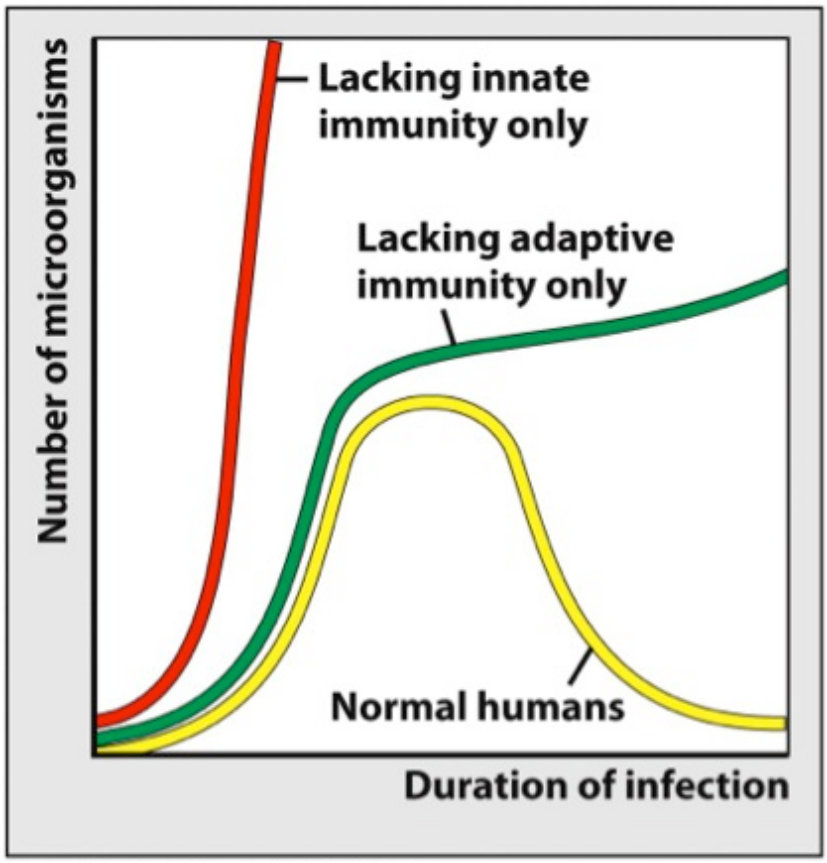

Figure 1.11 The Immune System, 3ed. (© Garland Science 2009)

Figure 2. The importance of having both innate and adaptive immune responses.

In a normal human (yellow line), the combined efforts of the innate and adaptive immune responses are necessary to successfully rid the host of infection. In a person who lacks innate immunity (red line), the number of pathogens increases dramatically and the infection goes unchecked. This is because without the innate immune response, the adaptive immune response cannot begin. In a person without adaptive immunity (green line) the infection is initially controlled by the innate immunity. However, often times the innate immunity is not able to completely get rid of the pathogen, thus the number of invading microorganisms remains relatively high and the infection persists. Image from Parham, 2009.

B Cells and Humoral Immunity

Produced and matured in the bone marrow, one of the primary lymphoid tissues, B cells are the lymphocytes in charge of eliminating extracellular pathogens (Parham, 2009). After maturation, mature B cells leave the bone marrow via the blood vessels, encounter pathogens in the lymph node, and become activated. B cells possess specialized receptors called B-cell receptors (BCRs), also known as immunoglobulins, used to recognize antigens (Parham, 2009). Therefore by definition, an antigen is a foreign substance that contains a structure recognized and bound by lymphocyte receptors (Parham, 2009; Atlan and Cohen, 1998). Formed from two different polypeptides called the heavy and light chain, the BCRs also have a region constant across all immunoglobulins, and a variable region that accounts for their diversity and ability to bind to different kinds of antigens. The B-cells and their receptors undergo various creation, selection and elimination processes during development and maturation to ensure that they only respond to foreign antigens and not self-proteins. Once in the secondary lymphoid organs, if naïve B cells encounter antigens for which they have affinity, they become activated and undergo clonal selection (with the assistance of T helper cells). This clonal selection results in the production of numerous copies of the activated B cell, all of which have slightly different BCRs after undergoing genetic rearrangement. After clonal selection, some of these B-cell copies then go on to become plasma cells, factories that produce antibodies

against that particular antigen (Parham, 2009). Others go on to become memory cells reserved for subsequent exposure to the same kind of pathogen. The antibodies produced by plasma cells can be found circulating in the blood and lymph and combating pathogens by: (i) covering the regions on the pathogen's surface necessary for attachment or spread thereby neutralizing the pathogen; (ii) acting as molecular tags that promote the phagocytosis of the pathogen by effector cells such as macrophages (Figure 3); and (iii) the recruitment of yet more immune cells to the site of infection (Parham, 2009).

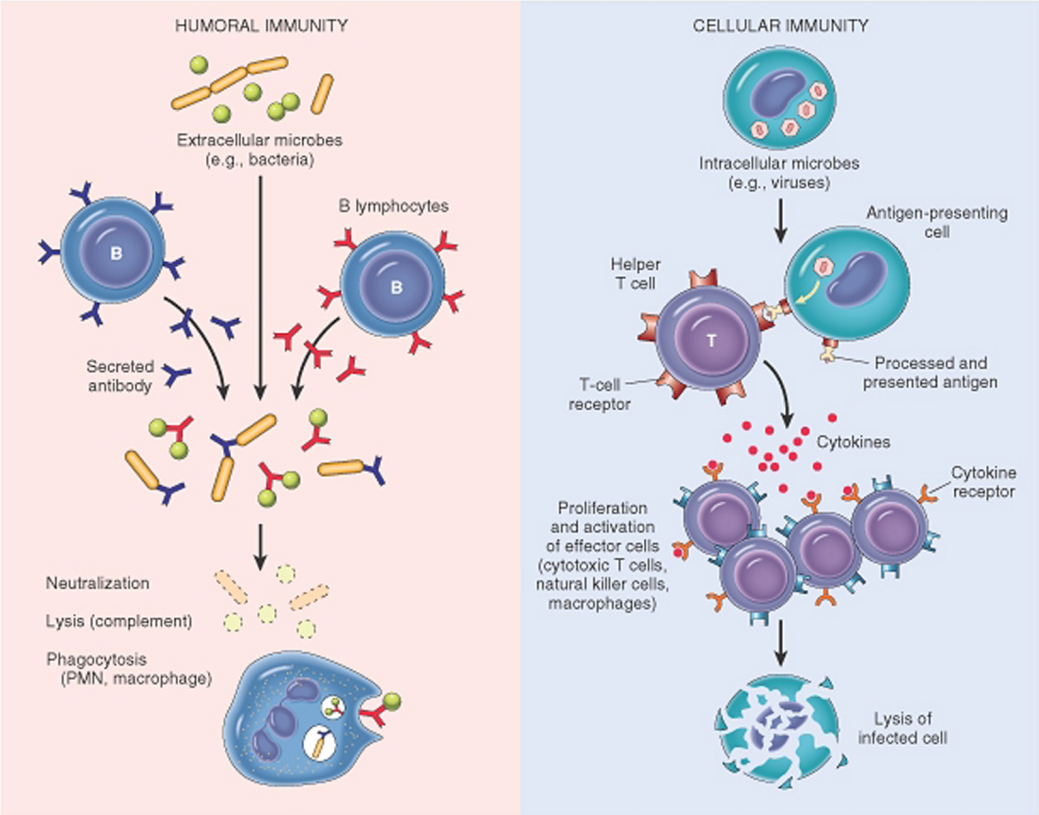

Figure 3. Overview of how Humoral and Cell-mediated Immunity work to combat infection.

The left panel shows the humoral response triggered by B cells interacting with extracellular pathogens such as bacteria. After pathogen encounter, B cells differentiate into antibody secreting cells. These antibodies bind to pathogens and facilitate their removal from the body. Cell mediated immunity involves various types of T cells which perform many functions. These functions include the secreting of soluble proteins that influence the activities of other cells of the immune system, and the direct killing of infected cells.

T cells and Cell-mediated Immunity

Unlike B cells that develop and mature in the bone marrow, after development, T cells migrate to another primary lymphoid tissue, the thymus, to complete maturation (Parham, 2009). In addition to developing T Cell receptors (TCRs) similar to the BCRs of B cells, during development in the thymus, the T cells also develop either CD4 or CD8 co-receptors (Parham, 2009). T cells are thus divided into CD4+ T cells, known as T helper cells because they aid in the development of other effector cells by the production of cytokines and by providing signal necessary for their proliferation; or CD8+ cytotoxic cells, which are responsible for eliminating cells infected with virus as well as other intracellular pathogens (Parham, 2009). However, TCRs and are different from BCRs in the sense that they cannot bind to antigen on their own but need the help of other cells known as antigen presenting cells (APCs) in order to bind to antigen and destroy it (Parham, 2009). This help is provided in the form of glycoproteins encoded by the genes in the major hisocompatibility complex (MHC) region of the genome, which are found on the surface of antigen presenting cells. These MHC molecules are genetically diverse and this diversity also contributes to the various ways in which antigens can be presented to T cells (Parham, 2009)

The CD8 co-receptor on the naïve CD8+ T cell, binds to a conserved site on the antigen-presenting cell's MHC Class I and becomes a cytotoxic T cell. The CD4 co-receptor on the naïve CD4+ binds to a conserved site on the APCs MHC Class II and becomes a T helper cell. It should be noted that CD4 cells primarily respond to peptides of extracellular pathogens presented via MHC Class II and CD8 cells typically respond to peptides of intracellular pathogens presented via MHC Class I (Figure 4).

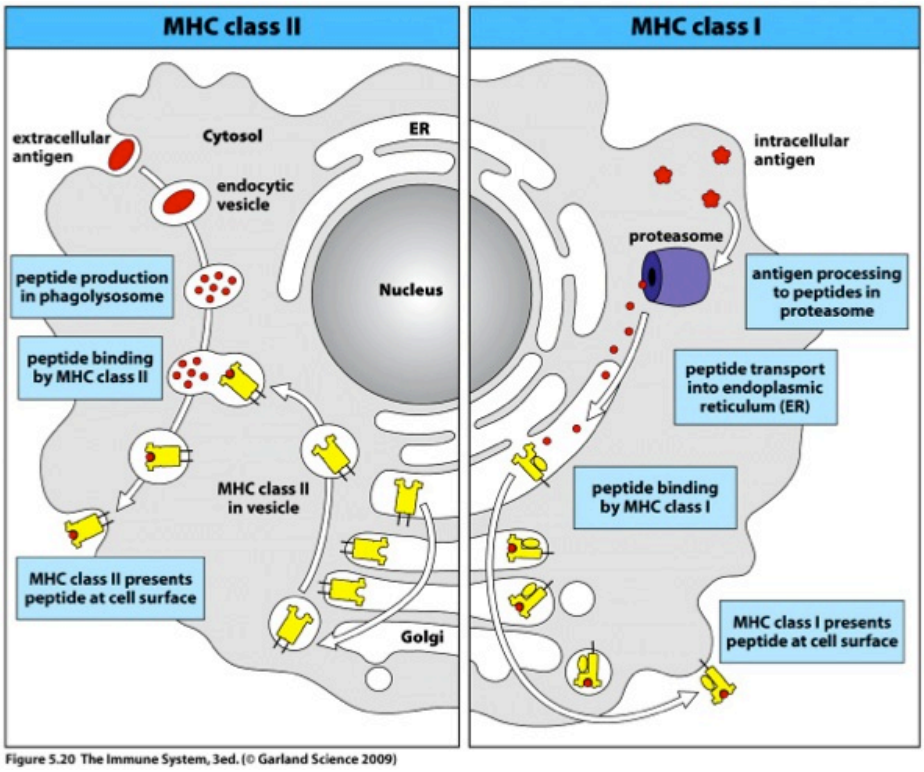

Figure 4. Processing of antigen peptides for presentation via MHC Class I and Class II molecules occur in different cellular compartments.

The left panel illustrates the processing of extracellular antigen into peptides, which are presented via MHC Class II. Extracellular pathogens are taken into vesicular system of the cell by endocytosis and are broken into peptides by proteases that reside in the vesicles. The endoplasmic reticulum (ER) and Golgi apparatus then transport MHC Class II molecules to the antigen processing vesicles where they meet up and bind to the antigenic peptides. The MHC Class II molecule then travels in an outgoing vesicle and presents the peptide at the cell surface. The right panel shows how intercellular antigens generated in the cytosol as a result of bacterial or viral infections, are processed into peptides and presented via MHC Class I. Intracellular antigens are broken down by the proteasome, and the resulting peptides are transported to the ER where meet and bind to MHC Class I molecules. The intracellular antigen:MHC Class I complex is then transported via the Golgi apparatus to be presented at the surface of the cell. Image by Parham, 2009.

All cells of the body except red blood cells possess MHC Class I and thus a virus infected cell's interaction with a CD8+ cytotoxic cell, would lead to the apoptosis of the targeted cell (van den Elsen *et al.*, 1998). However only professional antigen presenting cells (pAPCs) such as B cells, dendritic cells and macrophages, possess MHC Class II molecules and can interact with CD4+ cells. All T Cells including, CD8+ cells must first be activated by pAPCs. Professional antigen presenting cells digest extracellular pathogens in their lysosomes and present their peptides via MHC Class II, while their proteasomes digest intracellular pathogens found in the cytosol and present them via MHC Class I (Parham, 2009).

In addition to stimulation provided by the antigen:MHC complex on antigen presenting cells, naïve T cells also need co-stimulation by the same pAPC in order to become activated (Parham, 2009). This co-stimulation is achieved by the binding of another receptor on the surface of the T Cell called CD28 to the co-stimulatory molecules called B7 molecules, found on the surface of pAPCs (Parham, 2009). In the absence of co-stimulation even when a strong TCR - antigen:MHC complex bond has been, the T cell will remain inactivated (Parham, 2009). The presence of both stimulation by antigen:MHC complex and co-stimulation by CD28 - B7 interaction is necessary for T cell differentiation and

proliferation (Parham, 2009). Professional antigen presenting cells do not express co-stimulatory molecules in the absence of an infection.

Of the pAPC's, dendritic cells are the most potent in the adaptive immune response. This is because they are the most specialized APC's, producing antigens necessary for the activation of naïve T cells; they are cross presenters, presenting intracellular antigenic peptides via MHC Class I and extracellular antigenic peptides via Class II; they have strong co-stimulation abilities; and they are present throughout the body. Proteases in dendritic cells that chop up antigenic protein acquired from outside the cell include serine proteases, a family of proteases that will be discussed in more detail in the following pages.

Progression from HIV infection to AIDS

There are two forms of HIV: HIV-1, which is the more widely spread version of the virus and HIV-2, the virus strain more commonly found amongst West African patients (Gandhi and Campbell-Yesufu, 2011). In this paper, HIV means HIV-1 unless otherwise noted. HIV cripples the host's immune system by attacking and destroying macrophages, CD4+ T-helper lymphocytes, and dendritic cells (Weiss, 1993). Due to its status as a retrovirus, HIV infects target

cells by injecting its RNA into the host cell, converting its RNA to DNA, and injecting this DNA into the host cell's genome. The mechanism by which HIV achieves this end is by first binding to the CD4 receptor and either the CXCR4 or CCR5 co-receptors, then fusing its membrane with that of the host cell's (Brass *et al.*, 2008). After the fusion of the two membranes, the contents of the HIV viral core, which include the RNA genome plus reverse transcriptase, integrase, protease and other accessory proteins (Vif, Nef and Vpr), are released in to the host cell's cytoplasm (Brass *et al.*, 2008). These accessory proteins distinguish HIV from other retroviruses because in addition to working with the reverse transcriptase enzyme to generate the reverse transcription complex (Brass *et al.*, 2008), Vif and Vpr proteins suppress the antiviral activities of the host cell, while Nef and Vpr affect viral replication, propagation and persistence by regulating the activity, localization and abundance of host surface membrane proteins (Malim and Emerman, 2008). As illustrated by Figure 5, the reverse transcriptase complex synthesizes the viral double stranded cDNA and the enzyme integrase integrates this newly formed viral DNA into the host cell's DNA (Brass *et al.*, 2008). Once the viral DNA is integrated into the host's genome and produces new virons, they bud off from the cell and go on to infect new target cells (Frankel and Young, 1998). This process of the virus' invasion of target cells continues until the host's immune system is completely crippled, allowing for the invasion of opportunistic infections such as, but not limited to, common colds, Tuberculosis, Pneumonia (Masur *et al.*, 2002).

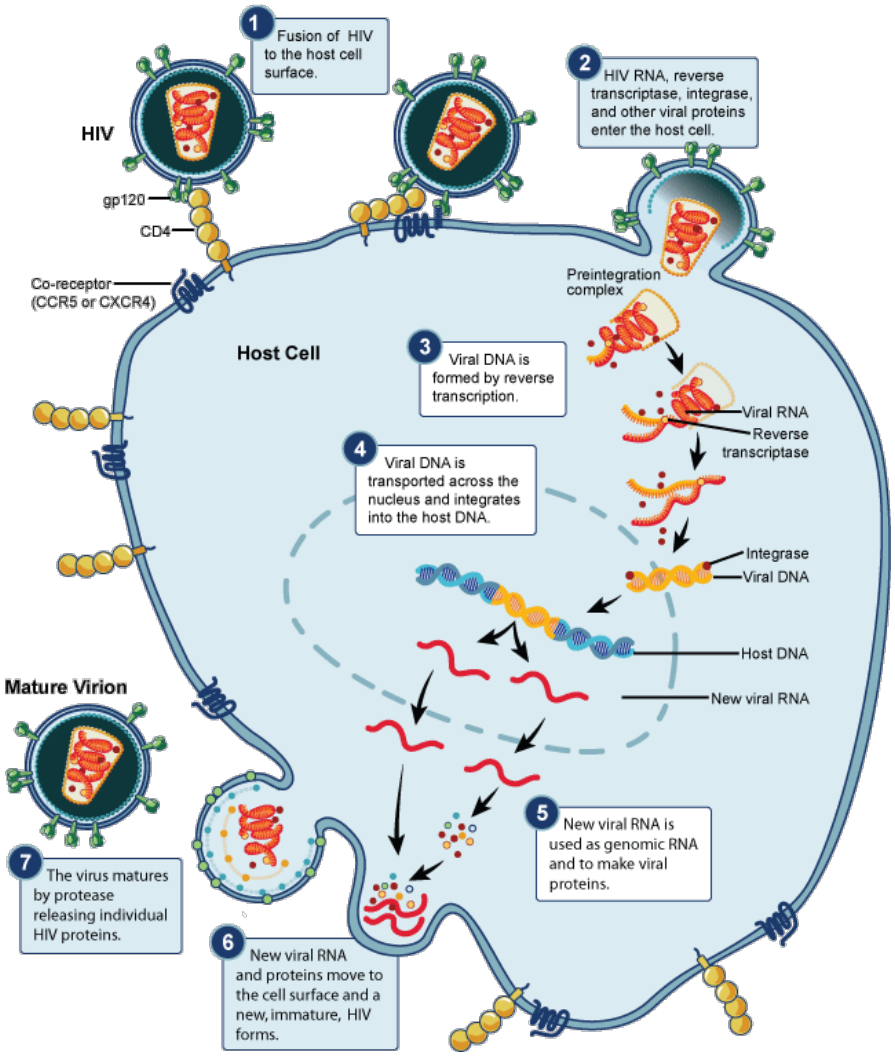

Figure 5. Replication cycle of HIV in infected cell.

HIV first fuses with the host cell membrane releasing HIV's RNA, reverse transcriptase, integrase and other viral proteins into the cytosol of the host's cell. Next, the viral RNA is transformed into DNA through reverse transcription. The newly formed viral DNA is then transported into the host's nucleus where it is integrated into the host's DNA. The viral DNA is can now be transcribed to form viral mRNA from which new viral proteins can be translated. New viral RNA and proteins migrate to the surface of the host's cell where they form new immature HIV forms. The mature virion buds off and goes on to infect other cells. Image from NIAID, 2010.

HIV is classified in the Retroviridae family as a lentivirus, a type of virus that induces a lifelong infection in the host by remaining latent for long periods of time, and resurfacing when the target cell is activated (Hunt, 2009). Infection with HIV often occurs after the transfer of contaminated bodily fluids such as blood, semen and vaginal fluids from an infected person to an uninfected individual. HIV infection is broken down into three stages: the primary infection, the asymptomatic or latent stage and the symptomatic chronic illness stage (Ik *et al.*, 2012). The primary stage of the infection is characterized by non-specific flu-like symptoms such as sore throat, fever and lymphadenopathy (swollen lymph nodes) and muscle pain (Fauci *et al.*, 1996). During this early stage of the infection, the body's immune system begins a HIV-specific immune response with APCs like dendritic cells and macrophages trapping the virus and presenting them to CD4+ T cells, simultaneously infecting and activating them (Baveja and Rewari, 2004). The CD4+ T cells in turn activate B cells and trigger the production of anti-HIV antibodies leading to seroconversion, a stage of infection when the antibodies against that infection are first detectable in the blood (Parham, 2009). The following latent stage can last as long ten years or more. During this period, the virus continues to infect and replicate in CD4+ T cells, slowly diminishing their numbers and weakening the host's immune system. The drop of the concentration of CD4+ T cells below 500cells/μl in blood signifies the end of the latent phase and the beginning of the symptomatic phase as this

reduction in CD4+ cells allows for the invasion of opportunistic pathogens. These opportunistic pathogens, which normally do not cause severe illnesses, further contribute to the depletion of the CD4+ cells. When the concentration of CD4+ T cells drops below 200 cells/μl the host is said to have progressed to full blown AIDS (Parham, 2009). At this stage, the individual diagnosed with AIDS often dies from opportunistic infections such as candidiasis and pneumonia.

A patient's progression to AIDS is highly dependent on a number of factors including education and access to anti-retroviral drugs, and the duration of this progression can range from 6 months to 20 or more (Ik *et al.*, 2012). However, there is a group of individuals whose HIV infection does not progress to AIDS despite their lack of use of precautionary measures such as anti-retroviral drugs and sometimes, safer sex practices (Blankson, 2010; Clerc *et al.*, 2009). This group of individuals, also known as long-term non-progressors (LTNPs) or elite controllers (Okulicz *et al.*, 2009), have become subjects of scientific research as investigating the mechanism(s) behind their control of viral infections and lack of progression to AIDS may provide clues valuable towards the design of possible HIV drugs and vaccines (Sáez-Cirión *et al.*, 2007).

The Murine Acquired Immunodeficiency Syndrome (MAIDS) Model

In a bid to better understand the intricacies behind HIV infection and AIDS progression, animal retroviruses that have similar characteristics to HIV have been identified and studied, giving rise to the development of animal models of HIV/AIDS. These animal models include the Simian Immunodeficiency Virus (SIV), which affects some species of African primates (Gardner *et al.*, 1989); Feline Immunodeficiency Virus infection of cats (Sparger *et al.*, 1989); HIV-1 infection of chimpanzees (Fultz *et al.*, 1986), rabbits (Kulaga *et al.*, 1989) and SCID mice reconstituted with a human immune system (Aldrovandi *et al.*, 1993); and Murine Leukemia Virus (MuLV) in mice. Of the aforementioned animal models, the MuLV virus, which progresses to Murine Acquired Immune Deficiency Syndrome (MAIDS) in some mouse strains, is one of the most easily applied. This is because some MuLV infected mice share similar symptoms such as lymphomas and susceptibility to opportunistic infections with humans infected with HIV (Mosier, 1996). In addition to this, some infected mice like the BALB/c strain never progress to MAIDS, while other strains such as the C57BL/6 are susceptible to the disease (Jolicoeur, 1991). Studying the mechanisms behind how the immune systems of these two strains of mice arrive at different outcomes post MuLV infection may help us understand what targets to aim for in the design for a vaccine against HIV, or help us uncover natural

immune pathways that could lead to HIV elimination and subsequent protective immunity against the virus. Other characteristics that make the MAIDS model an appealing animal model include, but are not limited to, it being a cheaper model due to its low biohazard risk and comparatively smaller containment and maintenance costs (Mosier, 1996); and the speed at which the disease progresses, allowing for quicker experiments. Studying the mechanisms behind how the immune systems of these two strains of mice arrive at different outcomes post MuLV infection may help us understand how HIV elite controllers achieve their resistance to AIDS.

The LP-BM5 isolate of MuLV used to induce MAIDS is a cocktail of three viruses: (i) BM5D, the 4.8 kbp disease causing replication-defective virus, (ii) MCFV, a B-tropic mink cell focus-inducing virus and (iii) BM5e, a replication-competent B-tropic ectopic virus (Casabianca *et al.*, 2003; Li and Green, 2006; Liang *et al.*, 1996). Although they are not responsible for the infection, the last two viruses, MCFV and BM5e, are helper viruses necessary for the proliferation of the virus as they provide the protein machinery required for the cell-to-cell spread of the etiological agent, BM5D (Chattopadhyay *et al.*, 1989). Depending on their interactions with the endogenous retroviruses (ERVs) already present in the genome of the mouse, the different viral components necessary to cause MAIDS may be responsible for the varying responses to the infection across mouse strains. Some strains are resistant to the infection and thus the disease, some are

able to get infected but overcome the infection and become resistant to the disease, while others are susceptible to both infection and resulting disease. Endogenous retroviruses (ERVs) are viral descendants of exogenous retroviruses that have infected certain animals, remained part of their genomes and have become major genomic components which contribute to the genetic diversity of the host but do not produce whole, infectious viruses (Bloomberg *et al.*, 2009; Bloomberg *et al.*, 2005; Whitelaw and Martin, 2001).

The MuLV susceptible C57BL/6 mouse strain possesses a defective germ-line encoded ERV with the potential to give rise to infectious MuLV (Mankan and Hornung, 2012). It is hypothesized by Beliharz *et al.* (2004) that ERVs expressed during development are recognized as self-antigens by the immune system. Thus, during an actual exogenous MuLV infection, MuLV foreign antigens are also recognized as self due to their genetic similarities to the ERVs present in the mouse genome. Conversely, it has been established that mouse strains without MuLV related ERVs control exogenous MuLV infection through a toll-like receptor 7 (TLR7) - dependent antibody response (Browne, 2011; Kane *et al.*, 2011).

In addition to the presence of ERVs, MAIDS susceptibility could also be influenced by the genetic diversity of MHC Class I and Class II molecules found on the professional antigen presenting cells (Makino *et al.*, 1990). Certain strains

of mice may express MHC Class I and II molecules that elicit more effective CD8+ cytotoxic T cell, CD4+ helper T cell and antibody immune responses. Although infection with the LP-BM5 isolate of MuLV induces immunological responses from B cells, the antibodies produced by B cell hyperactivity and clonal selection are not antigen specific and thus cannot produce an adequate immune response (Liang *et al.*, 1996). Even if the antibodies produced somehow neutralized the virons, the cell-mediated immunity is required to destroy infected cells to prevent the production of new virons.

MAIDS versus AIDS

Despite its many advantages, the MAIDS animal model as a tool for the study of HIV/AIDS is not without its flaws. Although the etiological agents of both AIDS and MAIDS are classified as retroviruses, they belong to a different genus, lentivirus (Jolicoeur, 1991) and c-type retrovirus (Beilharz *et al.*, 2004), respectively. Most importantly, unlike HIV that infects CD4+ T cells using the CD4 receptor (Mosier, 1996), MuLV infects B cells and macrophages via a different receptor (Beilharz *et al.*, 2004). Therefore while the drastic reduction of CD4+ T cells in the host is an indication of the progression of the HIV to AIDS, the CD4+ T cell count does not decline in MuLV infected mice. Nonetheless,

function in CD4+ T cells is progressively lost over time in both HIV and MuLV induced immune deficiencies.

Regardless of these differences, the MAIDS model remains a useful animal model because its overall susceptibility to progressive immune disruption by opportunistic infections, are shared with that of HIV induced AIDS (Mosier, 1996). In addition to these similarities, both MuLV and HIV infections induce CD4+ and CD8+ T cell anergy, limiting the ability of these important cells to properly respond to all sorts of infections (Mosier, 1996).

Previous Work in Stranford Lab

Although it has been established that T cells and the genes found in the major histocompatibility complex (MHC) play a vital role in the outcome of MuLV infection, recent studies have indicated that genetic differences in non-MHC loci are also associated with MAIDS resistance or susceptibility (Makino *et al.,* 1991). The current focus of research with the MAIDS model in the Stranford lab involves investigating non-MHC genes that may be associated with MAIDS resistance or susceptibility. A series of DNA microarray experiments that identified genes expressed in the spleen and lymph node (secondary lymphoid

organs) was conducted on both resistant and susceptible mice strains during the first week of MuLV infection. The results of these experiments revealed that the greatest difference in gene expression between the two strains occurred at 3 days post infection (Tepsuporn *et al.*, 2008).

Of the highly differentially expressed resistance-associated genes identified, several of them include genes that expressed between 100 and 600 fold difference levels (Tepsuporn *et al.*, 2008). Such genes include Chymotrypsinogen BI, Carboxypeptidase BI, Transmembrane Protease Serine 2 and Regenerating Islet-derived I (Tepsuporn *et al.*, 2008). These genes express serine proteases usually found in the pancreas and until recently, were unassociated with the immune response. However, it should be noted that many different proteases are found in proteasomes and immunoproteosomes; these both specifically break down proteins to be presented to T cells via MHC class I and Class II. Likewise, serine proteases have been identified as some of the enzymes responsible for the cascade of reactions that activate complement, a vital part of the innate immune response (Parham, 2009). Lastly, some of these proteases have been discovered to be involved in tissue microenvironment changes (Aimes *et al.*, 2003).

Serine Protease Family

Proteolytic enzymes are enzymes that hydrolyze peptide bonds that hold amino acids together. Enzymes that constitute the protease family are divided into four major subfamilies: (i) serine proteases, (ii) metalloproteases, (iii) aspartic preoteases and (iv) cysteine proteases, based on their catalytic sites (Safavi and Rostami, 2012). Serine proteases are characterized by the presence of three critical amino acids in their catalytic site (histidine, aspartate and a uniquely reactive serine side chain) (Kraut, 1977; Di Cera, 2009). They get their name from the involvement of the catalytic site serine in their proteolysis (Almonte and Sweatt, 2011). Serine proteases can be found across nature performing various functions in different kingdoms of cellular life, and in several viral genomes (Di Cera, 2009). In animals, serine proteases have been linked to numerous physiological processes such as blood clotting, cell death and tissue healing, as well as the immune response (Safavi and Rostami, 2012). Serine protease involvement in the immune system is multi-faceted. These enzymes are involved in the activation of complement (Parham, 2009) and they control inflammatory responses by regulating cytokine and chemokine production (Safavi and Rostami, 2012), in some cases converting them to their active forms (Ghayur *et al.*, 1997; Guma *et al.*, 2009). Serine proteases have also been implicated in the pathogenesis of specific auto-inflammatory diseases such as collagen-induced arthritis (Adkison *et al.*, 2002) and autoimmune diabetes in mice (Viret *et al.*, 2011). Lastly, serine

proteases such as Regenerating Islet-derived 1 (Reg1), one of the most highly expressed resistance-associated genes in both lymph nodes and spleen of animals in the MAIDS model, has been linked to capillary restructuring (Aimes *et al.*, 2003).

Regenerating Islet-derived 1 Protein

First discovered in regenerating pancreatic islets and isolated by Terazono *et al.* (1988), Reg1 is a gene encoding a 165 – 166 amino acid protein with identified mouse, rat and human homologs (Zhang *et al.*, 2003). Results of experiments comparing the volume of islet cells in Reg1 knockout mice and wild type have linked the Reg1 gene to the regenerative abilities of regenerating islet cells (Unno *et al.*, 2002). The Reg1 protein has been identified as a key factor in the replication and regeneration of insulin producing pancreatic β-cells (Okamoto, 1999), establishing its possible role in diabetes treatment therapies. In the same vein, the expression of the Reg1 protein has also been associated with the pathophysiology of several gastrointestinal conditions such as inflammatory bowel disease (Dieckgraefe *et al.*, 2002) and celiac disease (Planas *et al.*, 2011).

As in the case of celiac disease where it may serve as a potential biomarker for the disease (Planas *et al.*, 2011), the expression of Reg1 is not always a positive signal. However, in the mouse gastric system, Reg1 is associated with the healing of both stress induced and chemically induced gastric ulcers (Fukuhara *et al.*, 2010). This healing is characterized by the production of Reg1 protein by enterochromaffin-like (ECL) cells, the prominent endocrine cell type found in the acid producing part of the stomach usually associated with the production of histamine (Håkanson *et al.*, 1994). Induced by the release of CINC2β, the mouse equivalent of human Interleukin 8 – a pro-inflammatory cytokine (Colditz *et al.*, 1989; Larsen *et al.*, 1989) – ECL cells in the periphery of the gastric ulcer lacerations produce Reg1, which influences the proliferation of gastric progenitor cells (Fukui *et al.*, 1998). In an experiment to confirm the role of Reg1 in the healing of mouse gastric ulcers, Fukuhara *et al* (2010) studied both Reg1-trangenic mice and wild-type mice, and came to the conclusion that that the expression of Reg1 protein promotes ulcer healing by encouraging progenitor cell growth. This conclusion is supported by an observed increase in Reg1 detection and a corresponding accelerated healing of ulcer lacerations in the Reg1-transgenic mice compared with the wild-type mice (Fukuhara *et al.*, 2010).

Other studies have established that the expression of the Reg1 protein is not limited to pancreatic and gastrointestinal sites. The presence of Reg1 has been connected to neuronal sprouting and regeneration in the mature mouse

brain (de la Monte *et al.*, 1990; Xu *et al.*, 1995; Van Ba *et al.*, 2012) and the mRNA of its identified receptor, EXTL3, has been found expressed in the liver, kidney, adrenal gland and pituitary gland (Kobayashi *et al.*, 2008). These findings lend support to Tepsuporn *et al.*'s (2008) theory suggesting the possible role of Reg1 protein in cell types that participate in the immune response. Therefore, further investigations into the presence of Reg1 protein in the secondary lymphoid organs of MuLV infected mice may provide pivotal insight into understanding the underlying mechanisms within the immune system that give rise to the development of MAIDS.

Proposed Studies

Tepsuporn *et al.* (2008) propose the possible involvement of proteolytic enzymes and chemokines identified in their study in the physiological restructuring of lymphoid organs during an immune response. They hypothesize that these enzymes and chemokines play a role in the development of new blood and lymph vessels, and the regulation of the Th2 pathway for leukocyte trafficking signals, all of which could support eradication of the virus and resistance to MAIDS. Conversely, the absence of these resistance-associated genes in the early stages of infection may result in pathogenic signals and a lack of

remodeling favoring MAIDS. This project hopes to investigate the presence of the protein product of one of the resistance-associated genes, Regenerating Islet-derived I, and determine if the differential expression of the gene in the resistance BALB/c mice versus the susceptible BL/6 mice also translates to a differential protein expression. The results of this study may confirm whether or not the expression of Reg1 protein is associated with MAIDS. Future studies could be aimed at uncovering which of the immune system's effector cells produces this protein and whether this protein plays a role in virus eradication and/or disease resistance.

MATERIALS & METHODS

Reg1 ELISA

The Enzyme-linked immunosorbent assay (ELISA) is a biochemical assay system that is used to quantify either antigens or antibodies (Reen, 1994). ELISA assays can be configured in two ways: (i) direct assays using either an antigen-enzyme conjugate or an antibody-enzyme conjugate, and (ii) a noncompetitive assay that employs a sandwich technique where the antigen of interest is nestled between a capture antibody and a detection antibody conjugated with an indicator enzyme (Reen, 1994).

In the absence of a commercially available Reg1 ELISA kit, Akalu's (2012) protocol for designing an indirect indoleamine 2, 3-dioxygenease (IDO) ELISA technique was adapted in the designing of a Reg1 ELISA. In this indirect ELISA, a microplate is coated with the antigen of interest and primary antibody specific for this antigen is added to the plate. After the primary antibody binds to the antigen, an enzyme-conjugated detection secondary antibody specific for the primary antibody is introduced. Following the binding of the secondary antibody to the antigen-primary antibody complex, a chromogenic substrate is added and a color change develops in the wells. This color change is quantified using a UV-

Vis spectrophotometer and its associated computer software. Figure 6 illustrates the basic steps involved in an indirect ELISA.

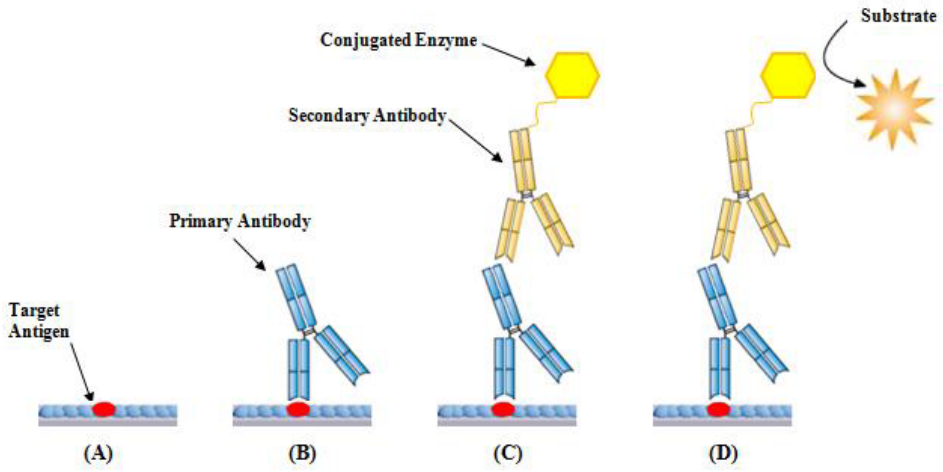

Figure 6. An Illustration of an Indirect ELISA process.

(A) In this ELISA technique, the wells of the plate are first coated with the antigen of interest. (B) An unlabeled primary capture antibody specific for the target antigen binds to it. (C) An enzyme-conjugated secondary antibody specific for the primary antibody binds to the primary antibody's fragment crystallization region (Fc region). (D) Protein detection is achieved when a substrate is added to the wells and it cleaves enzyme conjugated to the secondary antibody, resulting in a chromogenic product. The intensity of this chromogenic product is quantified by a spectrophotometer and the appropriate software is used to translate its absorbance values to protein concentration. Image by Yemsratch Akalu (2012)

Designing Reg1 ELISA protocol

All reagents and enzymes were freshly prepared and kept on ice throughout the experiment. Recombinant mouse Reg1 protein obtained at 0.280mg/mL from R&D systems (available upon request) was diluted to 2,000pg/mL in carbonate coating buffer (0.159g Na_2CO_3, 0.35g $NaHCO_3$, in 100ml of diH_2O, pH 9.6) creating a stock solution. Eleven two-fold serial dilutions of rReg1 ranging from 2,000pg/mL to 1.9531pg/mL were prepared from this stock solution and 100µl aliquots of each serial dilution were added down each column of wells of a clear 96-well high affinity ELISA plate (BD Falcon #353279). Likewise, 100µl of coating buffer *sans* rReg1 protein was added to the last column of wells to serve as the negative control (Figure 8). These known concentrations are used to obtain a standard curve necessary for the analysis of the unknown samples.

The plate coated with standard rReg1 protein serial dilutions was covered with parafilm and incubated at 4°C overnight. After the overnight incubation, the coated wells were washed three times with PBST (0.05% Tween-20 in 1x autoclaved PBS; 1x PBS = 0.156g NaH_2PO_4, 8.5g NaCl, 1.6g Na_2HPO_4 in 1L diH_2O, pH 7.0 – 7.2). To minimize non-specific binding of antibodies to the wells, each well was then blocked with 250µl assay diluent, 1x R&D Reagent Diluent Concentrate 2 (Cat. DY995), diluted in milliQ water from the 10x stock.

The plate was then covered with parafilm and incubated at room temperature on a shaker (Multi-purpose Rotator, Thermo Scientific) for 2 hours. After incubation, the plate was washed three times with PBST.

To determine what concentrations of primary antibody and Horseradish peroxidase (HRP) conjugated secondary antibody would result in the optimum standard curve, different concentrations of these antibodies were tested in different combinations. The primary antibody, lyophilized anti-mouse Reg1 affinity purified sheep IgG (R&D Systems, cat. AF1657) reconstituted to 0.2mg/mL in sterile PBS (pH 7.4), was diluted to 0.8μg/mL, and 0.4 μg/mL in assay diluent and 100 μL of each primary antibody solution was added the appropriate wells as described in Figure 7. Plate was then covered with parafilm and incubated at room temperature for 1 hour. The plate was again washed three times with PBST. Secondary antibody, Horseradish peroxidase (HRP) conjugated anti-sheep IgG (R&D Systems, Cat. HAF016) was prepared 1:100 and 1:200 in assay diluent, 100 μL of the appropriate concentration was added to the appropriate well (Figure 7).

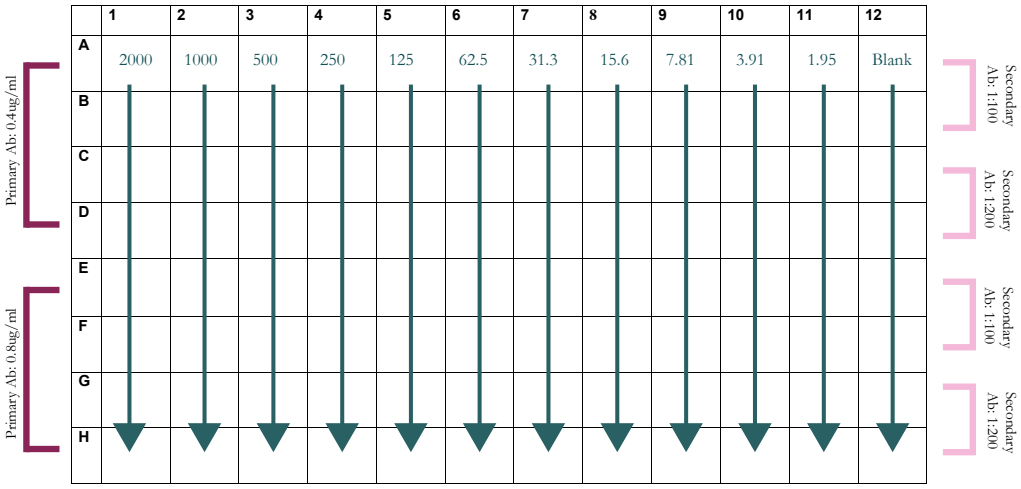

Figure 7. Ninety-six well ELISA plate template showing how different concentrations of primary and secondary antibodies were tested.

Two-fold serial dilutions of standard rReg1 were put in to wells starting with 2000pg/mL of Reg1 down column 1, to 1.95pg/mL down column 11. Coating buffer was put in all the wells in column 12. After an overnight incubation at 4°C and several washes, 0.4ug/mL of primary anti-mouse Reg1 affinity purified sheep IgG was put in all the wells of rows A to D and 0.8ug/mL of the same antibody was put in wells of rows E to H. After several washes, secondary antibody, Horseradish peroxidase (HRP) conjugated anti-sheep IgG diluted 1: 100, was put in wells of rows A, B and E, F. A second dilution, 1:200, of the same secondary antibody was put in wells of rows C, D and G, H. Thus, each primary antibody concentrations were tested with each secondary antibody concentration.

After an hour-long incubation at room temperature, the plate was washed five times with PBST, and 100µL of a 1:1 mixture of substrate solutions A and B (BD Biosciences OptEIA TMB Substrate Reagent Set, cat. 555214) was added to

each washed well. After the addition of the substrate, the plate was incubated uncovered and in the dark for 15mins. Lastly, 50μL of stop solution, 1M H_3PO_4, was added to each well to stop the enzyme-substrate reaction. The plate was then gently swirled to ensure the complete mixing of the stop solution with the enzyme-substrate complexes, and the optical density of each well was measured using a microplate reader (SpectraMax, Molecular Devices), set to 450nm with wavelength correction set to 570nm.

Obtaining a Standard Curve

To obtain the best standard curve, absorbance values of the serially diluted Reg1 protein tagged with various primary and secondary antibody concentrations were plotted against their corresponding known concentrations using different graphing equations. The graphing equations used were the straight-line equation, quadratic equation, exponential equation, log-log equation and the 4-parameter logistic curve equation.

Mice and MuLV Infection

Six to seven week old female mice of both BALB/c and C57BL/6 strains were obtained from Taconic Labs, New York. The mice were housed in the Mount Holyoke College Animal Facility and handled according to the National Institute of Health Guidelines for the Care and Use of Laboratory Animals. Four mice of each strain were given an intraperitoneal injection of LP-BM5 isolate of Murine Leukemia Virus (virus titer, 1.5×10^3 PFU/ml) and were sacrificed three and a half days after exposure to the virus. Similarly, four uninfected mice from each strain were sacrificed to serve as the naïve controls.

Organ Isolation, Cell Lysis and Sample Preparation

The spleen from each sacrificed mouse was retrieved, cut into small pieces and crushed in the presence of 1mL cold lysis buffer (1x protease inhibitor cocktail from BD BaculoGold in PBS with 0.05% Triton X-100 at pH 7.4). Similarly, the axillary, brachial and inguinal lymph nodes from each animal were retrieved, pooled together and placed in 0.5mL cold lysis buffer. The mesenteric lymph nodes of each animal were also retrieved but were placed in a separate vial containing 0.5mL cold lysis buffer. The locations of harvested tissues are highlighted in Figure 8. All the tissue samples were homogenized carefully for about 30 seconds at ¾ speed using a polytron homogenizer. The homogenized

tissue samples were then transferred into appropriately labeled 2mL centrifuge tubes and centrifuged at 12,000g for 10 minutes at 4°C. Without disrupting the resulting pellet, the supernatant was removed and stored in 100µl aliquots in 1.5mL tubes labeled accordingly and stored at -20°C until needed.

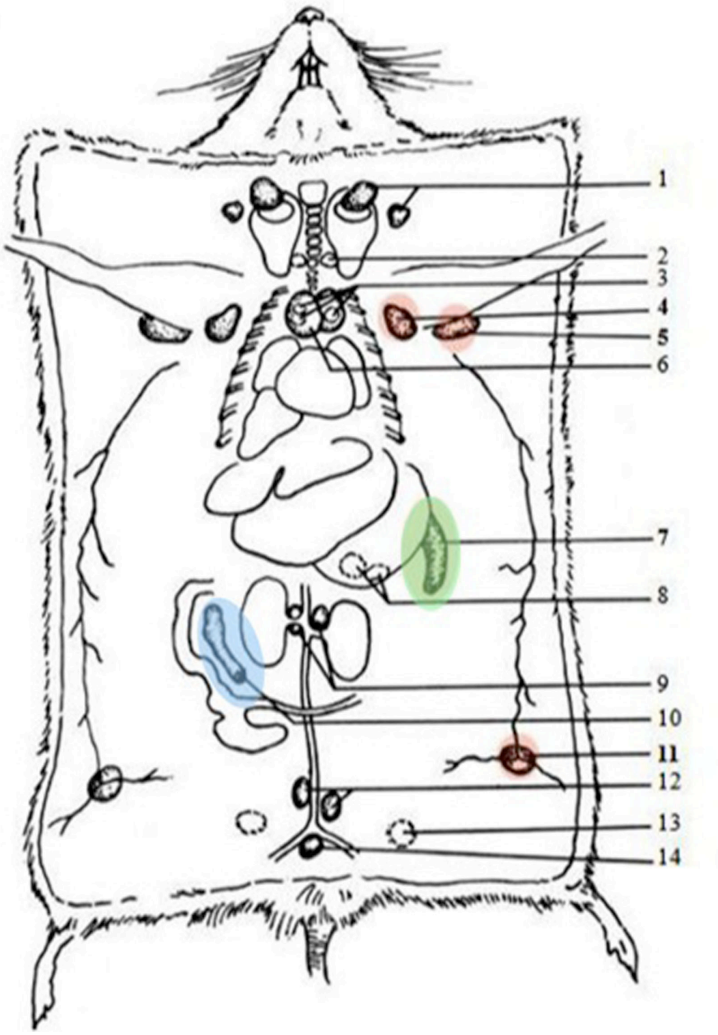

Figure 8. Schematic representation of the locations of secondary lymphoid organs in *Mus musculus* relative to other organs.

The image shows the locations of all the lymph nodes, which are numbered 1 – 6 and 8 – 14, and the spleen (7). All the lymph nodes lying away from the center of the body are bilateral and are therefore found symmetrically on either side of the body. The different groups of secondary lymphoid organs examined in this study are; the peripheral axillary lymph nodes (4), brachial lymph nodes (5) and inguinal lymph nodes (11) (highlighted red); the mesenteric lymph nodes (10) (highlighted blue); and the spleen (7) (highlighted green). Image adapted from Dunn, 1954.

Testing Mouse Tissue Samples

Once the appropriate concentrations of primary and secondary antibodies were determined, and the optimum standard curve achieved, the experiment was repeated with mouse tissue samples. The serial dilutions of rReg1 as described above were plated on to a clear 96-well high affinity ELISA plate (BD Falcon #353279) with 100µl of each concentration in triplicate wells down each column (Figure 9). The last column in the plate was coated with 100µl of the coating buffer in triplicate wells to serve as the standard protein blank.

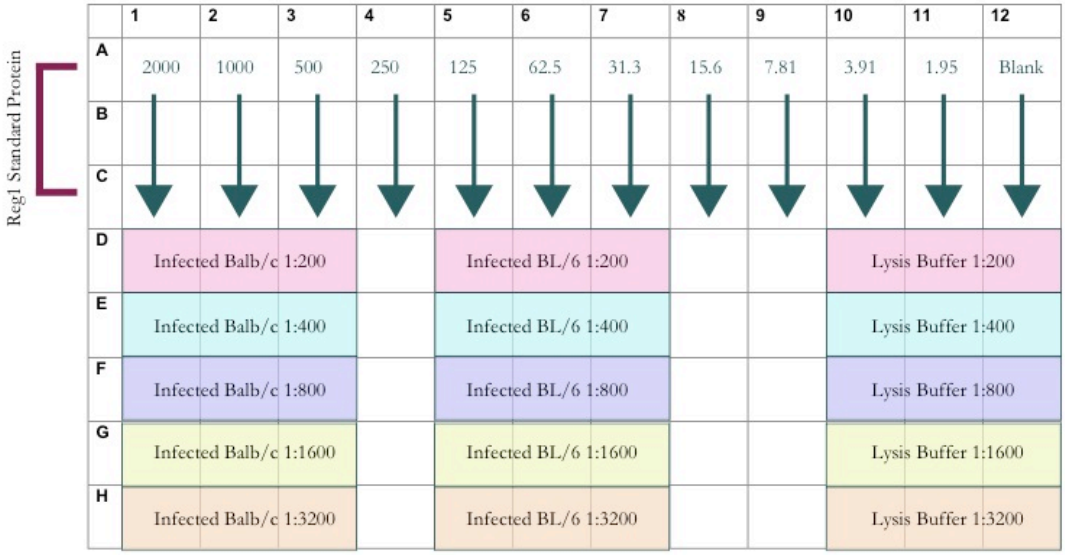

Figure 9. Ninety-six well ELISA plate template showing how different dilutions of tissue samples were tested.

Two-fold serial dilutions of standard rReg1 were put in to triplicate wells starting with 2000pg/mL in column 1, to 1.95pg/mL in column 11. Likewise, coating buffer was put in triplicate wells in column 12. Samples diluted 1:200 were placed in triplicate wells across row D with one well separating samples from the two different mice strains. The lysis buffer, also diluted 1:200, was put in triplicate wells in row D but starting two wells after the last sample well. In the same manner, samples and lysis buffer diluted 1:400, 1:800, 1:1600 and 1:3200 were placed in triplicate wells in rows E to H.

Spleen samples from one infected mice of both strains were diluted in coating buffer in different concentrations ranging from 1:200 to 1:3200. A hundred microliters of each resulting solution was plated in triplicate wells (Figure 9). Lysis buffer used in the isolation and separation of the samples were diluted similarly in coating buffer and 100μl of each resulting solution was plated in triplicate wells to serve a blank for the samples.

The plate with the standard Reg1 protein and the samples was covered with parafilm and incubated at 4°C overnight. After the overnight incubation, the plate was treated in the steps as described in the *Designing an ELISA Protocol* section except that this time, only the determined primary and secondary antibody concentrations were used.

The plate was then read with a microplate reader and each well's absorbance value was recorded. The absorbance values of the serially diluted standard rReg1 protein were plotted against their known concentrations using the graphing equation determined in the earlier part of this experiment, and a standard curve was obtained. This standard curve was used to determine the unknown concentrations of the spleen samples, and the best dilutions of the samples were chosen to be used as the sample dilutions going forward.

The harvested tissue samples of all sacrificed mice were then tested. Each tissue type and the corresponding state of infection were assigned to a 96-well microplate. Therefore, there were six plates with different categories: naïve spleen, infected spleen, naïve lymph node, infected lymph node, naïve mesenteric lymph node and infected mesenteric lymph node. Since four mice belong in each group of strain and infection state, there were 8 mouse samples on each plate.

The rReg1 standard dilutions were plated in triplicates as described earlier and so was the standard blank of coating buffer. The tissue sample for each mouse was diluted with the earlier determined best dilution factor and the diluted samples were plated in triplicates. The appropriately diluted lysis buffer was also put in triplicate wells and this served as the sample blank (Figure 10). The plates were incubated overnight at 4°C and the treated with the procedure describe in *Designing an ELISA Protocol* section. However for the testing of the samples, only concentrations of primary and secondary antibodies determined to produce the best standard curve were used in the experiment. Figure 10 illustrates how the mouse samples were plated.

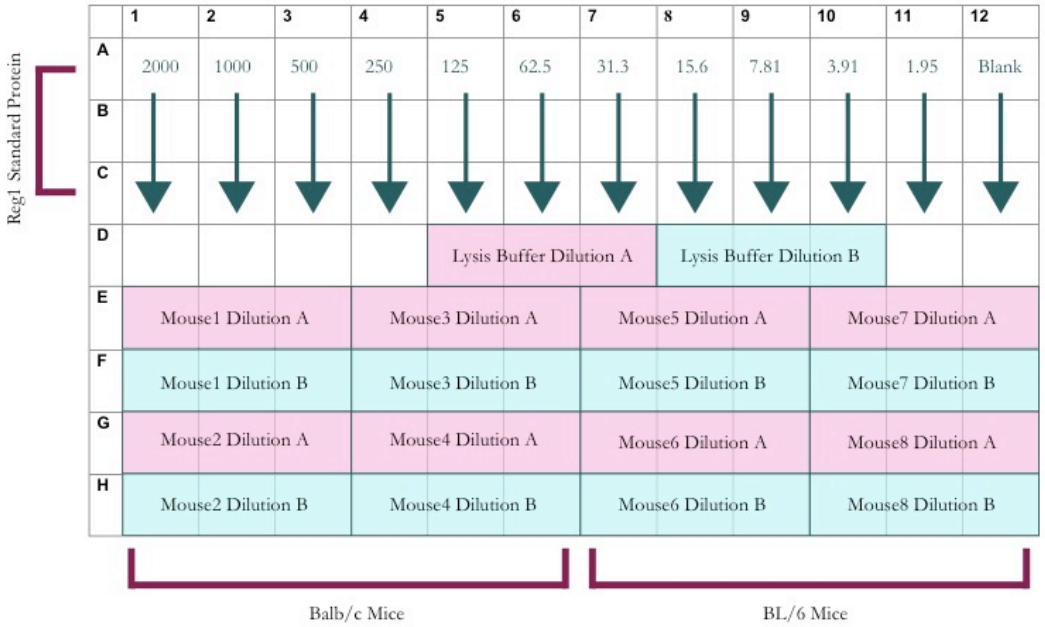

Figure 10. Ninety-six well ELISA plate template showing how tissue samples of different mice were tested for Reg1.

Two-fold serial dilutions of standard rReg1 were put in to triplicate wells starting from 2000pg/mL in column 1, to 1.95pg/mL in column 11. Likewise, coating buffer was put in triplicate wells in column 12. Tissue samples of each mouse were diluted in the dilution ratios specified, and these diluted samples were plated in triplicate wells per dilution. Therefore each mouse sample was diluted twice. The lysis buffer was also diluted with the same dilution ratios as the samples and this served as the sample blank.

The plate was read by the microplate reader and the absorbance value of each well was recorded. With the aid of the bioanalytical software, SoftMax Pro (version 5.1), the graphing equation determined as the best fit for this experiment was used to plot the absorbance values of the standard Reg1 protein against their known concentrations. This plot resulted in the standard curve by which the unknown concentration of each diluted mouse sample was determined also using SoftMax Pro.

Bradford Assay

To provide a basis for comparing the concentration of Reg1 present in each sample to the total amount of protein present in that sample, a Bradford assay was conducted on each mouse tissue sample. A Bradford assay is biochemical assay that uses color change and absorbance values of Coomassie Brilliant Blue dye to measure the concentration of protein in a solution (Bradford, 1976).

Standard BSA (bovine serum albumin) protein provided with a Coomassie (Bradford) Protein Assay Kit (Thermo Scientific, Product No. 23200) at 2mg/mL was serially diluted with 1x PBS to concentrations 2000ug/ml, 1500ug/mL, 1000ug/mL, 750ug/mL, 500ug/mL, 375ug/mL, 250ug/mL, 187.5ug/mL,

125ug/mL, 62.5ug/mL, and 31.25ug/mL. Ten microliters of each serially diluted protein concentration was plated in triplicate wells and so was 1x PBS *sans* standard BSA, which served as the blank. Spleen and Mesenteric lymph nodes of naïve and infected mice of both strains were diluted 1:10 in 1x PBS. Tissue types were assigned to separate microplates and 10ul of each diluted sample was plated in triplicates as shown in Figure 11.

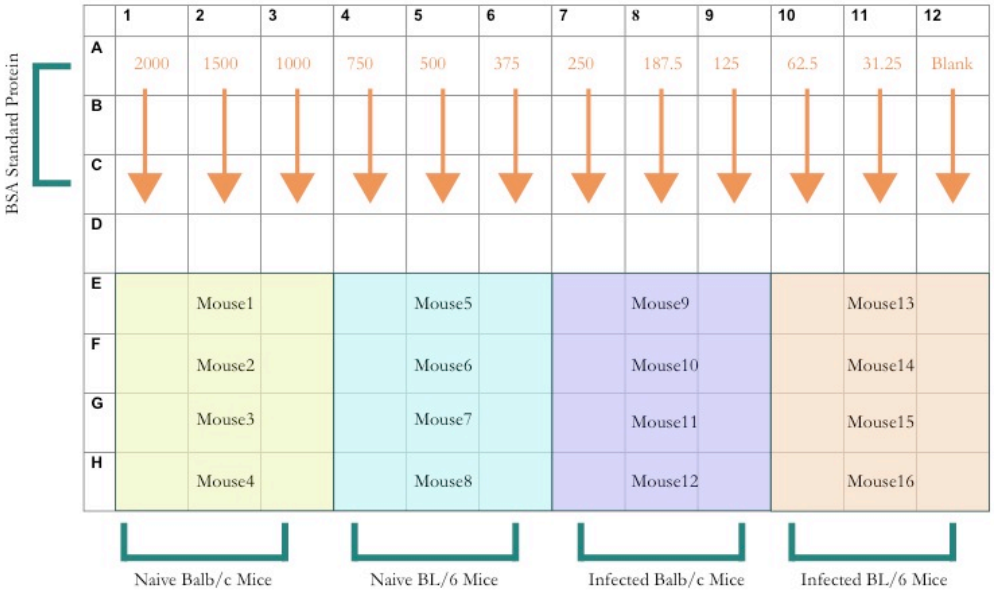

Figure 11. Ninety-six well ELISA plate template showing how total protein concentrations of tissue samples of each mouse was tested using a Bradford Assay.

Serially diluted Standard BSA protein was put into triplicate wells starting from 2000ug/mL in column 1, to 31.25ug/mL in column 11. The first three wells down Column 12 contain 1x PBS, which served as the protein blank. Tissues sample from each mouse diluted 1:10 in 1x PBS was put in triplicate wells.

After the standard protein concentrations and the samples were added to their respective wells on the microplate, 250ul of Coomassie Protein Assay Reagent was added to each well. The plate was then mixed using the shaker function on the microplate reader, and incubated at room temperature for 10mins. Following the incubation, each plate was read at 595nm and their absorbance values recorded. Using SoftMax Pro, the absorbance values of the BSA standard dilutions were plotted against their known concentrations using the four-parameter logistic fit equation, and a standard curve was obtained. With the help of SoftMax Pro, the BSA standard curve was used to determine the total protein concentration of each mouse tissue sample. The total concentration of protein from lymph node samples was obtained from a colleague (Roses, 2013)

Data Analysis

Once the concentration of Reg1 (pg/mL) was determined for each sample at each dilution, it was then divided by the total amount of protein (ug/mL) in that same sample. Statistical analysis was done on the results using a univariate analysis of variance (ANOVA), with a two-way factorial experimental design on the statistical analysis software, IBM SPSS Statistics. The dependent variable was the concentration of Reg1 per microgram of total protein, and the

independent variables, which were also the two factors in the two-way factorial, were strain (Balb/c or BL/6) and health (naïve or infected). ANOVA is a collection of statistical models that analyses the difference between the means of groups, determines whether the means of multiple sample groups are equal and determines the variation within each group. It does so by testing a null hypothesis that the error variance of the dependent variable is equal across groups. Thus the null hypothesis for this experiment was that there is no difference in the expression of Reg1 protein between different groups of different mouse strains and health states. Statistical significance was ascribed to p values less than 0.03.

To check that the data conformed to the assumptions of ANOVA, residuals were examined in both Q-Q and scatter plots. To fulfill the conditions of ANOVA, the concentration of Reg1 per microgram of total protein for each tissue sample was transformed using its natural logarithm. This was done for each tissue at each sample dilution.

Two tailed *t*-tests were also conducted to determine significant difference between two groups. This test was done to compare naïve Balb/c and BL/6 animals; infected Balb/c and BL/6 animals; Balb/c naïve and Balb/c infected animals; and BL/6 naïve and BL/6 infected animals. These *t*-tests were conducted for each tissue type sample at each concentration and statistical significance was ascribed to p values less than 0.05.

RESULTS

Standard Curve Determination

Due to the unavailability of a commercial Reg1 ELISA kit, one of the main objectives of this study was to design an ELISA assay that quantifies the amount of Reg1 in mouse tissue samples. To obtain a suitable standard curve to measure the concentrations of unknown samples, different mathematical graphing equations were used to plot the absorbance values of the standard recombinant Reg1 protein against their corresponding known concentrations. The standard curve generated using a linear fit gave an R^2 value of 0.278; a Log-Log fit an R^2 value of 0.608; and for a quadratic, R^2 value was 0.515. A fourth standard curve (Figure 12) was generated using an exponential fit with equation $y = A + B \times (1 - exp^{(-\frac{x}{c})})$. This gave a higher R^2 value of 0.987 but like the previous graphing equations, it was a poor fit for the data.

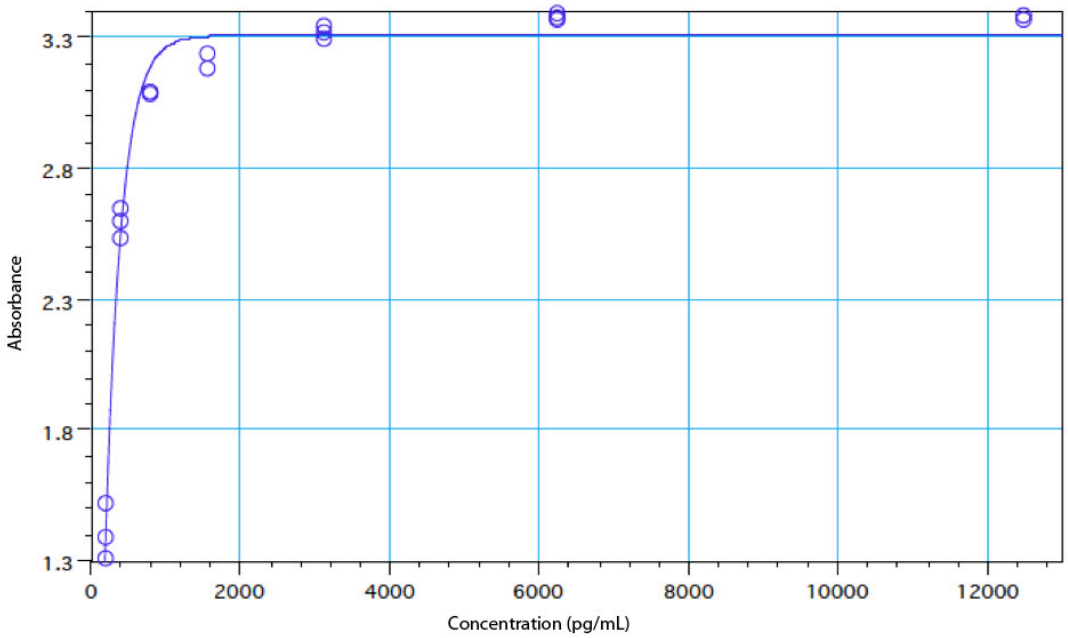

Figure 12. Graph showing standard curve of recombinant Reg1 generated with exponential fit.

Absorbance values of serial dilutions of rReg1 standards were plotted against their known concentrations. Equation is $y = A + B \times \left(1 - exp^{\left(\frac{-x}{c}\right)}\right)$, where A = -1.34, B = 4.65, C = 217. R^2 value of graph is 0.987.

Lastly, a fourth standard curve (Figure 13) was generated using the 4-parameter logistic regression fit with equation $y = \frac{A-D}{1+\left(\frac{x}{C}\right)^B} + D$. This gave the best fit for the data with an R^2 value of 0.995.

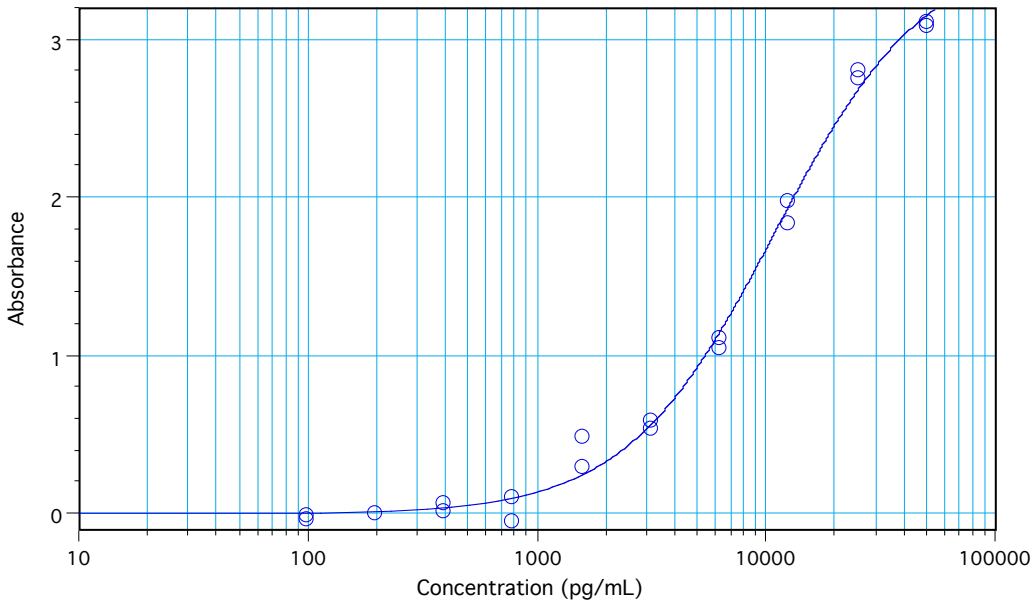

Figure 13. Graph showing standard curve of recombinant Reg1 generated with 4-Parameter Logistic Regression fit.

Absorbance values of serial dilutions of rReg1 standards were plotted against their known concentrations. Equation is $y = \frac{A-D}{1+\left(\frac{x}{C}\right)^B} + D$, where A = -0.0061, B = 1.33, C = 1.09×10^4. R^2 value of graph is 0.995.

The 4-parameter logistic regression curve was chosen as the graphing equation to be used going forward because: it gave the highest R^2 value of 0.995, which indicates the best curve fit; and when back calculated, the obtained concentration values of the Reg1 standard were a close match with their known concentrations. Most commercially available ELISA kits are developed using the 4-parameter curve and the linear portion of the curve is used to determine the standard protein concentrations included in such kits. The 4-parameter mathematical graphing model fit is characterized by a sigmoidal shape that fits the top and bottom plateaus of the curve (Cardillo, 2013). The resulting graph has an inflection point and the fit takes into consideration the maximum and minimum asymptotes, and the slope (Figure 14).

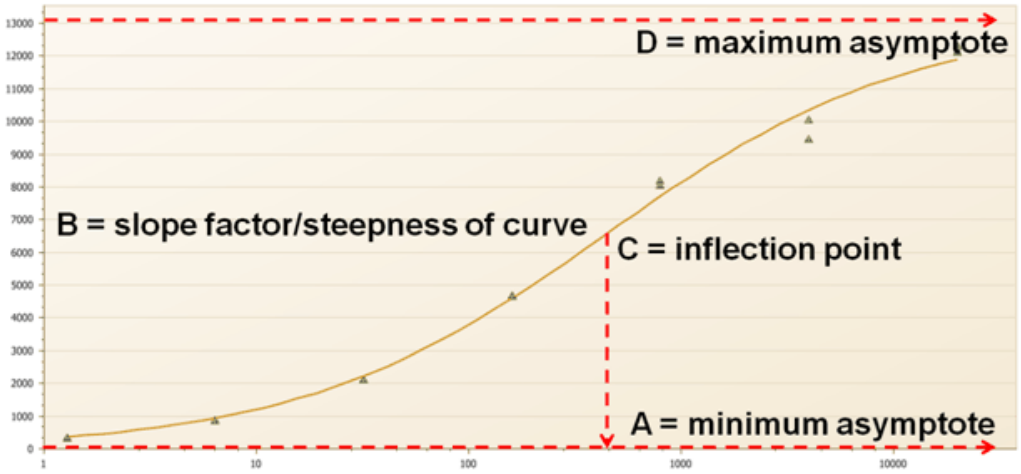

Figure 14. Typical 4-Parameter Logistic Curve showing the four parameters taken into consideration when calculating the equation.

These four parameters are: A = the minimum asymptote where the response value is at 0 concentration; B = the steepness of the curve, this can either be positive or negative; C = the inflection point, the point on the graph where the curvature changes directions or signs; D = the maximum asymptote, the response value for the infinite standard concentration. A typical 4-parameter logistic curve has a sigmoid shape where the concave upward and concave downward portions of the graph are separated by a linear portion, the slope. Image from Ma, 2010.

Determining Antibody Concentrations

Once the appropriate equation for generating the Reg1 standard curve was determined, it was used in the testing of different primary and secondary antibody concentrations illustrated in Figure 15. The R^2 values generated using the 4-parameter logistic curve fit for the testing of these primary and secondary antibody concentrations were: $R^2 = 0.974$ for primary antibody concentration 0.4ug/mL and secondary antibody concentration 1:100 (Rows A and B, Figure 15); $R^2 = 0.990$ for primary antibody concentration 0.4ug/mL and secondary antibody concentration 1:200 (Rows C and D, Figure 15); $R^2 = 0.995$ for primary antibody concentration 0.8ug/mL and secondary antibody concentration 1:100 (Rows E and F, Figure 15); $R^2 = 0.989$ for primary antibody concentration 0.8ug/mL and secondary antibody concentration 1:200 (Rows G and H, Figure 15). The concentrations 0.8ug/ml for primary antibody, and 1:100 for secondary antibody, had the standard curve with the best R^2 value of 0.995 and thus these concentrations were chosen as the optimal concentration for future experiments.

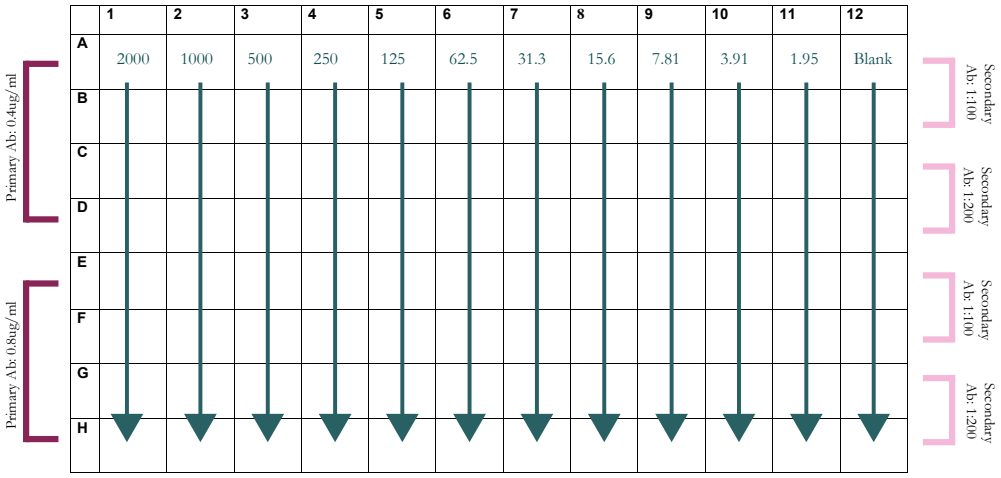

Figure 15. Ninety-six well ELISA plate template showing how different concentrations of primary and secondary antibodies were tested.

Two-fold serial dilutions of standard rReg1 were put in to wells starting with 2000pg/mL of Reg1 down column 1, to 1.95pg/mL down column 11. Coating buffer was put in all the wells in column 12. After an overnight incubation at 4°C and several washes, 0.4ug/mL of primary anti-mouse Reg1 affinity purified sheep IgG was put in all the wells of rows A to D and 0.8ug/mL of the same antibody was put in wells of rows E to H. After several washes, secondary antibody, Horseradish peroxidase (HRP) conjugated anti-sheep IgG diluted 1: 100, was put in wells of rows A, B and E, F. A second dilution, 1:200, of the same secondary antibody was put in wells of rows C, D and G, H. Thus, each primary antibody concentrations were tested with each secondary antibody concentration.

Determining the Dilutions for Mouse Tissue Samples

Mouse spleen tissue samples from one infected mouse of each strain were diluted with dilution factors 1:200, 1:400, 1:800, 1:1600 and 1:3200, and the optimal primary and secondary antibody concentrations obtained from the pervious experiment were used to run an initial trial test for the amount of Reg1 in these dilutions (Figure 9). Table 1 shows the mean absorbance values for each dilution of an infected mouse's tissue sample, from each strain.

Table 1. Mean absorbance values of triplicate mouse spleen samples diluted at various dilution factors.

Sample Dilution	BALB/c Absorbance Values	BL/6 Absorbance Values
1:200	1.526	1.433
1:400	1.433	1.182
1:800	1.176	0.643
1:1600	0.565	0.277
1:3200	0.252	0.139

Unlike a sandwich ELISA assay where the use of capture antibodies ensure that only the protein of interest is captured, an indirect assay has no capture antibody, hence, all protein in the sample is 'captured' on the plate. Thus, to avoid the interference of other proteins and their non-specific binding to the antibodies, the samples for indirect ELISA assays have to be diluted considerably. Starting with dilutions at 1:200, samples were diluted in half down to 1:3200. Therefore, the samples diluted at 1:400 were half as concentrated as samples diluted 1:200, and samples diluted 1:800 were half as concentrated as samples diluted 1:400. However, most of the absorbance values of these various sample dilutions did not reflect this change in concentration (Table 1). It was expected that the absorbance values of samples diluted 1:200 would be double the absorbance values of samples diluted 1:400, and absorbance values of samples diluted 1:400 would be double the absorbance values of samples diluted 1:800. Unfortunately, this was not the case as samples diluted 1:200, 1:400 and 1:800 had absorbance values that fell within the same 0.4 range (Table 1). Dilution factors 1:800 and 1:1600 were chosen as the dilution factors to be used to test the mouse tissue samples because it their absorbance values showed that there was less interference of non-specific protein in the assay. The absorbance values of samples diluted 1:800 and 1:1600 also reflected the changes in their concentrations. The absorbance values of 1:800 diluted samples were twice those of the 1:1600 samples. Another factor that was taken into consideration was the

slope of the 4-parameter curve. The absorbance values of the chosen dilution factors had to fall within the linear portion of the graph as the concentration values calculated from the upper and lower portion of the sigmoid shaped curve have greater errors associated with them (Gee, *et al.*, 1996).

Determining the Unknown Concentrations of Mouse Tissue Samples

Analysis of Reg1 protein expression was done on spleen, pooled peripheral lymph node and mesenteric lymph node tissues obtained from 4 mice of each strain and condition. Therefore, there were samples from 4 different animals in each category of BALB/c naïve, BALB/c infected, BL/6 naïve and BL/6 infected. The tissue samples were diluted 1:800 and 1:1600, the optimum dilution factors determined in previous experiments.

For lysis buffer absorbance values in the positive range, their calculated protein concentration was subtracted from the similarly diluted mouse tissue sample. This resulted in Reg1 protein concentrations that accounted for the possible effects of the lysis buffer. The mean Reg1 protein concentration in the tissue of interest of all 4 animals in each group was assessed using the bar graph

function in Microsoft Excel. The Bradford Assay revealed the total protein concentration in each mouse sample, and the Reg1 concentration in each mouse sample was then corrected by dividing the Reg1 concentration by the total protein concentration in the sample. This resulted in the concentration of Reg1 in picograms per microgram of protein. The Bradford corrected Reg1 concentration of each mouse was averaged within a group and the results were assessed using a bar graph with standard errors bars shown. This was done for each tissue type at each dilution.

Spleen

Figure 16 shows the means of uncorrected Reg1 mouse samples per group in a bar chart. This bar chart compares the mean Reg1 concentrations of two strains of mice, BALB/c resistant and BL/6 susceptible, against each other at each health condition and at each sample dilution factor. For samples diluted at 1:800, the mean Reg1 concentration in spleen tissue in the BALB/c naïve group was about 60,000pg/mL, and the mean Reg1 concentration in the BL/6 naïve group was about 50,000pg/mL. Infected tissue samples at the same dilution had about a 5-fold increase in Reg1 concentration than the naïve tissue samples. The mean Reg1 concentration of 1:800 diluted spleen tissues in the infected BALB/c

group was about 300,000pg/mL and the mean in the infected BL/6 group was about 200,000pg/mL.

For samples diluted at 1:1600, the mean Reg1 concentration of spleen tissue in the BALB/c naïve group was about 80,000pg/mL, while in the BL/6 naïve group it was about 60,000pg/mL. At this dilution, infected tissue samples showed an increase in Reg1 by almost a 10-fold when comparing the naïve tissues with the infected tissues. The mean Reg1 concentration in spleen tissue of the infected BALB/c group was about 600,000pg/mL, and about 500,000pg/mL in infected BL/6 group.

The comparison between naive BALB/c and BL/6 mouse spleen samples diluted at 1:800 yielded a p value of 0.47, while the comparison of infected BALB/c and infected BL/6 at the same dilution yielded a p value of 0.13. These p values greater than 0.05 tell us that there is no statistical difference between these groups. Comparing the naïve BALB/c spleen samples diluted at 1:800 with the infected group of the same mouse strain diluted similarly yielded a p value of 0.0009, and a comparison of naïve BL/6 samples with infected BL/6 samples yielded a p value of 0.0001. These p values lower than 0.05 indicate that the difference between the compared groups was statistically significant and that

infection causes a statistically significant change in Reg1 concentration in both animal strains.

The p values of the comparison of samples diluted at 1:1600 were similar to those diluted 1:800 and lead us to arrive at the same statistical conclusions.

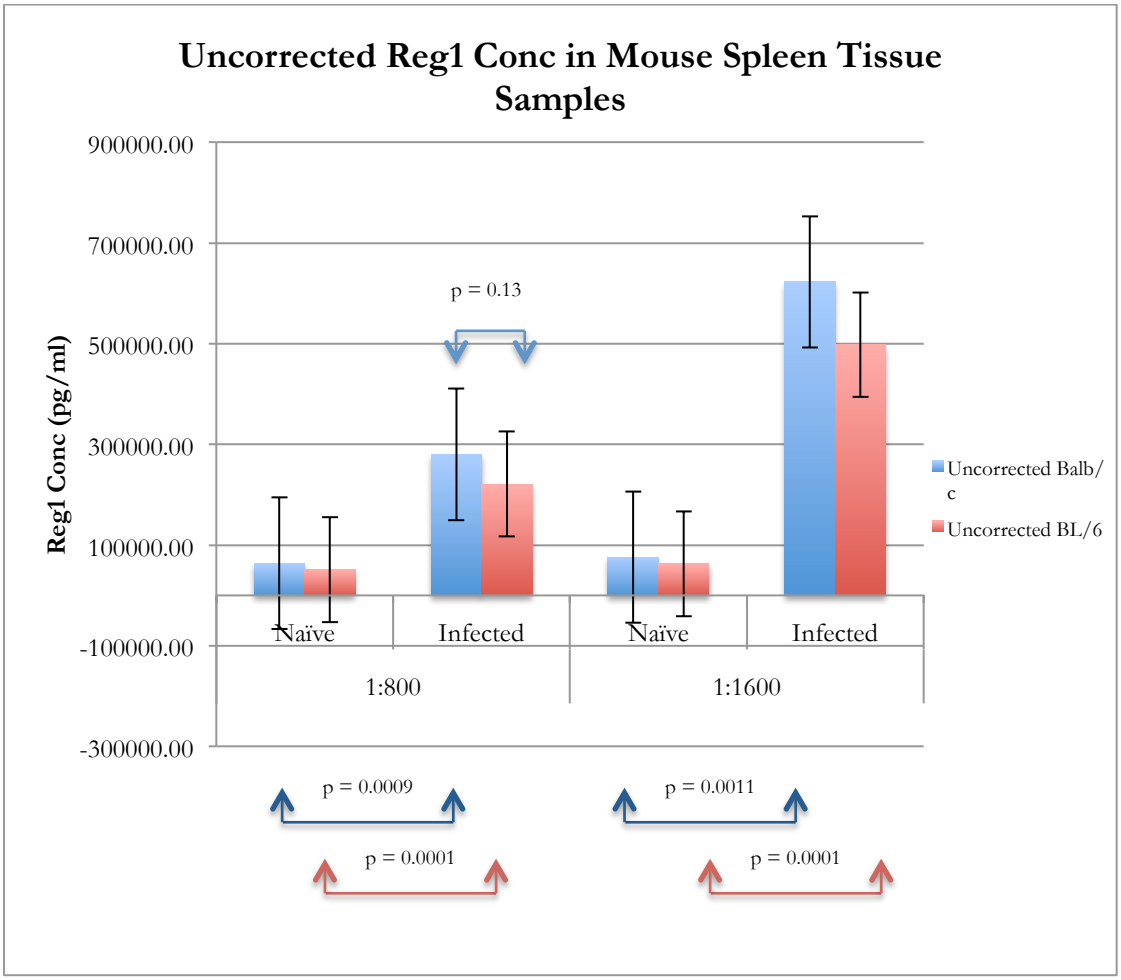

Figure 16. Bar graph comparing the means of uncorrected Reg1 concentration in mouse spleen tissue samples in each group.

Infected samples diluted at 1:800 seemed to have 5 times as more Reg1 protein than the naïve samples at the same dilution. Infected samples diluted 1:1600 had a larger difference in Reg1 concentration, as they seemed to have about 10 times as much Reg1 as naïve samples of the same dilution. In both dilutions, naïve BALB/c seems to be making more than naïve BL/6, and infected BALB/c seems to be making more than infected BL/6. However, the high p values comparing these two groups indicate that the difference is not statistically significant.

The Bradford Assay provided a way to calculate the amount of Reg1 present in each sample relative to the total amount of protein present in that sample. In Figure 17, the bar chart compares the mean Bradford corrected Reg1 concentrations of the two strains of mice against each other, at each health condition and at each sample dilution factor. For samples diluted at 1:800, the mean Bradford corrected Reg1 concentration of spleen tissue in the BALB/c naïve group was about 15pg/ug of total protein, and 17pg/ug of total protein in the BL/6 naïve group. Infected tissue samples had about a 2-fold increase in Reg1 concentration compared to the naïve tissue samples. The mean Bradford Corrected Reg1 concentration of spleen tissue in the infected BALB/c group was about 34pg/ug of total protein, and about 33pg/ug of total protein in the infected BL/6 group.

For samples diluted at 1:1600, the mean Bradford Corrected Reg1 concentration of spleen tissue in the BALB/c naïve group was about 19pg/ug, while it was about 22pg/ug in the BL/6 naïve group. Bradford Corrected Reg1 concentration in infected tissue samples increased by almost 4-fold at the same dilution. The mean Bradford Corrected Reg1 concentration of spleen tissue in the infected BALB/c group was about 75pg/ug while the infected BL/6 group had a mean Bradford Corrected Reg1 concentration of about 73pg/ug.

The comparison between naive BALB/c and BL/6 mouse spleen samples diluted at 1:800 yielded a p value of 0.64, while the comparison of infected BALB/c and infected BL/6 at the same dilution yielded a p value of 0.93. Both p values indicate that the difference between the compared groups is not statistically significant. A comparison of the naïve BALB/c and the infected BALB/c spleen samples diluted at 1:800 yielded a p value of 0.025. This indicates that the difference between the two groups is statistically significant and that health condition has a significant effect on the amount of Reg1 found in BALB/c mice. The comparison of naïve BL/6 samples with infected BL/6 samples also diluted at 1:800 yielded a p value of 0.10, indicating that the difference between these two groups is not statistically significant. Thus for these two groups, infection does not cause a statistically significant change in Reg1 concentration.

The p values of the comparison of samples diluted at 1:1600 were similar to those diluted 1:800 and lead to the same conclusion of statistical significance.

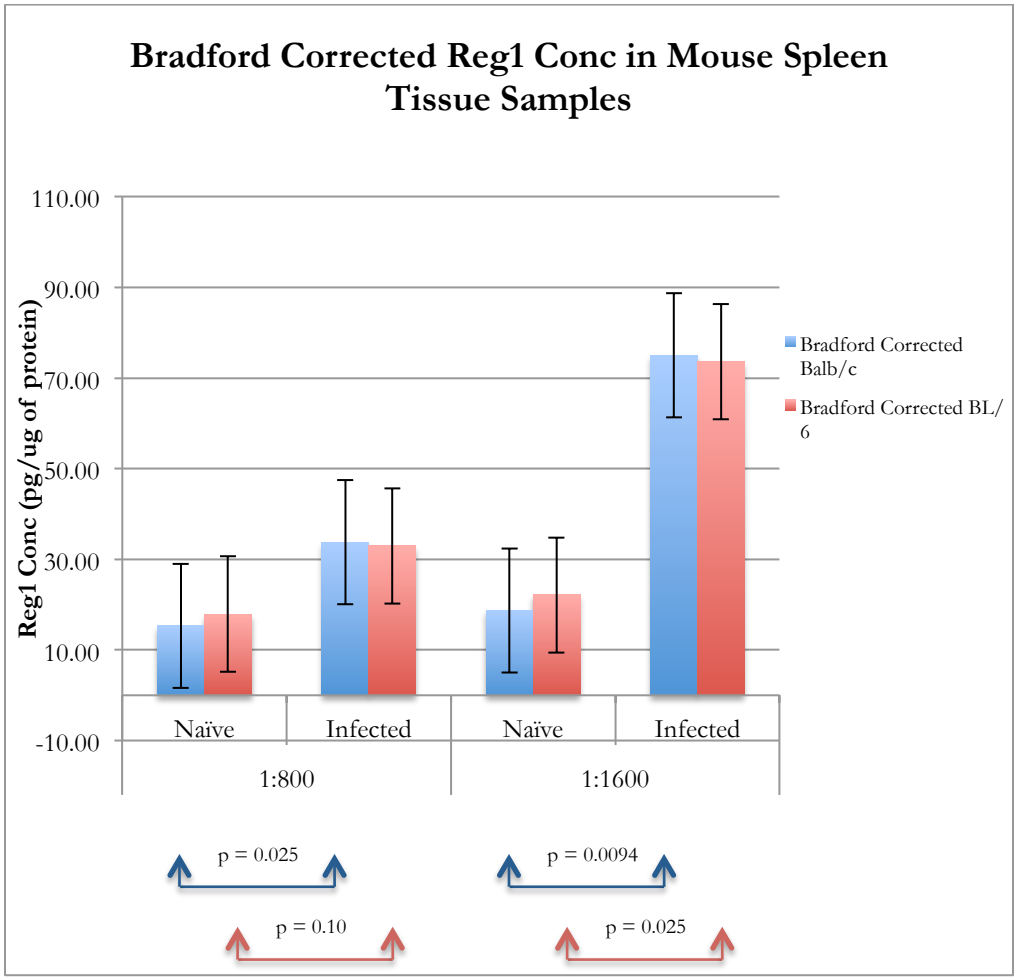

Figure 17. Bar graph comparing the means of Bradford Corrected Reg1 concentration in mouse spleen tissue samples in each group.

Infected samples diluted at 1:800 seemed to have 2 times as more Reg1 protein than the naïve samples at the same dilution. Infected samples diluted 1:1600 had a larger difference in Reg1 concentration, as they seemed to have about 4 times as much Reg1 as naïve samples of the same dilution. In both dilutions, naïve BL/6 seems to be making more than naïve BALB/c, and infected BALB/c seems to be making more than infected BL/6. However, the high p values comparing these two groups indicate that the difference is not statistically significant.

The Bradford corrected spleen sample data was analyzed using analysis of variance (ANOVA) with a two-way factorial experiment design. The two factors (independent variables) were mouse strain, which had two levels: BALB/c and BL/6; and health condition which also had two levels: naïve and infected. The response (dependent variable) was the concentration of Reg1 per microgram of protein. To meet the ANOVA assumptions, and control for how far set the Reg1 concentration values may be spread out (variance) the Bradford corrected data was transformed into its natural logarithmic values. The normality of the transformed data was then confirmed by examining the data's residuals in Q-Q and scatter plots, and comparing them to the Q-Q and scatter plots of the untransformed data. Q-Q plots are used to examine data distribution. If most of the points fall on or around a straight line, the data is said to be normal. This process of data transformation was done for Bradford corrected samples at both concentrations 1:800 and 1:1600.

Figure 18 shows an interaction graph that compares the effect of both experimental factors on the concentration of mouse spleen samples diluted at 1:800. At the naïve condition, the BL/6 strain seems to have a higher Bradford Corrected Reg1 concentration than the BALB/c strain. The opposite seems to be the case at the infected state. At 3.5 days post infection, the BALB/c strain seems to have a higher Reg1 concentration than the BL/6. However, the p value (p =

0.684) obtained from the ANOVA analysis indicates that the difference between strains is not statistically significant. When comparing the Reg1 concentrations of spleen samples across health conditions, both mouse strains have more Bradford corrected Reg1 when infected than they do when uninfected. The p value ($p = 0.0003$) obtained from the ANOVA analysis confirms that the health condition (naïve or infected) has a significant effect on the concentration of Reg1 in mouse spleen samples. Therefore, the results of the ANOVA confirm the results of previously conducted group *t*-tests. The ANOVA analysis also tested for interaction between the two factors, and the p value of 0.470 indicates that there is no statistical interaction. This means that the effect of one factor on Reg1 concentration is independent of the second factor.

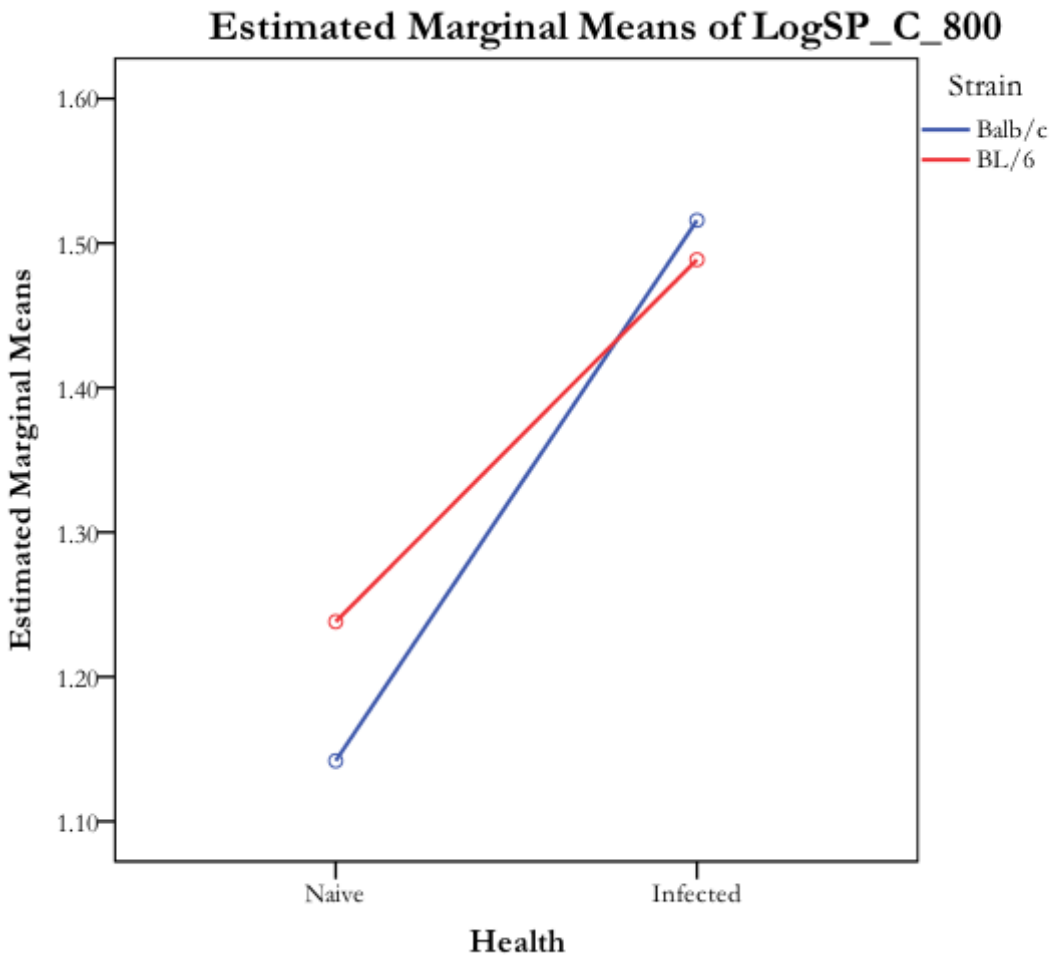

Figure 18. Interaction graph showing how the two factors (health condition and strain) affect the response (Log of Bradford Corrected Reg1 concentration) of spleen samples diluted at 1:800.

Bradford Corrected Reg1 concentration in spleen samples increases from naïve to infected for both animal strains. However, this there is no significant difference between the two mouse strains at each health condition.

The results of the ANOVA analysis of spleen samples diluted 1:1600 were very similar to samples diluted 1:800 and lead us to the same statistical conclusions.

Lymph Node

The Reg1 concentration of the pooled brachial, inguinal and axillary lymph nodes of each animal were subject to the same statistical analysis as the spleen samples. Figure 19 is a bar chart that shows the means of uncorrected Reg1 concentrations in mouse lymph node samples in each group. This bar chart compares the mean Reg1 concentrations of two strains of mice against each other at each health condition and at each sample dilution factor. For samples diluted at 1:800, the mean Reg1 concentration of lymph node tissue in the BALB/c naïve group was about 40,000pg/mL, and about 20,000pg/mL in the BL/6 group. Infected tissue samples at the same dilution had about a 9-fold increase in Reg1 concentration compared to the naïve tissue samples. The mean Reg1 concentration of 1:800 diluted lymph node tissues in the infected BALB/c group was about 180,000pg/mL and the mean concentration in the infected BL/6 group was about 170,000pg/mL.

For samples diluted at 1:1600, the mean Reg1 concentration of lymph node tissue in the BALB/c naïve group was about 37,000pg/mL, while the mean Reg1 concentration of lymph node tissue in the BL/6 naïve group was about 30,000pg/mL. Infected tissue samples increased almost by a 10-fold in Reg1 concentration compared to the naïve tissues in the same strain. The mean Reg1 concentration of lymph node tissue in the infected BALB/c group was about 270,000pg/mL, and about 220,000pg/mL in the infected BL/6 group.

The p values resulting from the comparison between different sample groups is summarized in Table 2. Of the groups compared, only the comparisons between naïve and infected samples within the same strains yielded p values lower than 0.05. Therefore the difference in Reg1 concentration between strains at each health condition was not statistically significant. However, in both strains, the difference in Reg1 concentration from naïve to infected conditions was statistically significant indicating that infection lead to a significant change in the concentration of Reg1 in these samples.

Table 2. P values resulting from the comparison of uncorrected Reg1 concentration values of different sample groups of lymph node tissue

Dilution	Group Comparisons	P values
1:800	Naïve BALB/c and Naïve BL/6	0.060
	Infected B BALB/c and Infected BL/6	0.83
	Naïve BALB/c and Infected BALB/c	0.0001
	Naïve BL/6 and Infected BL/6	0.0026
1:1600	Naïve BALB/c and Naïve BL/6	0.57
	Infected B BALB/c and Infected BL/6	0.31
	Naïve BALB/c and Infected BALB/c	0.0003
	Naïve BL/6 and Infected BL/6	0.0008

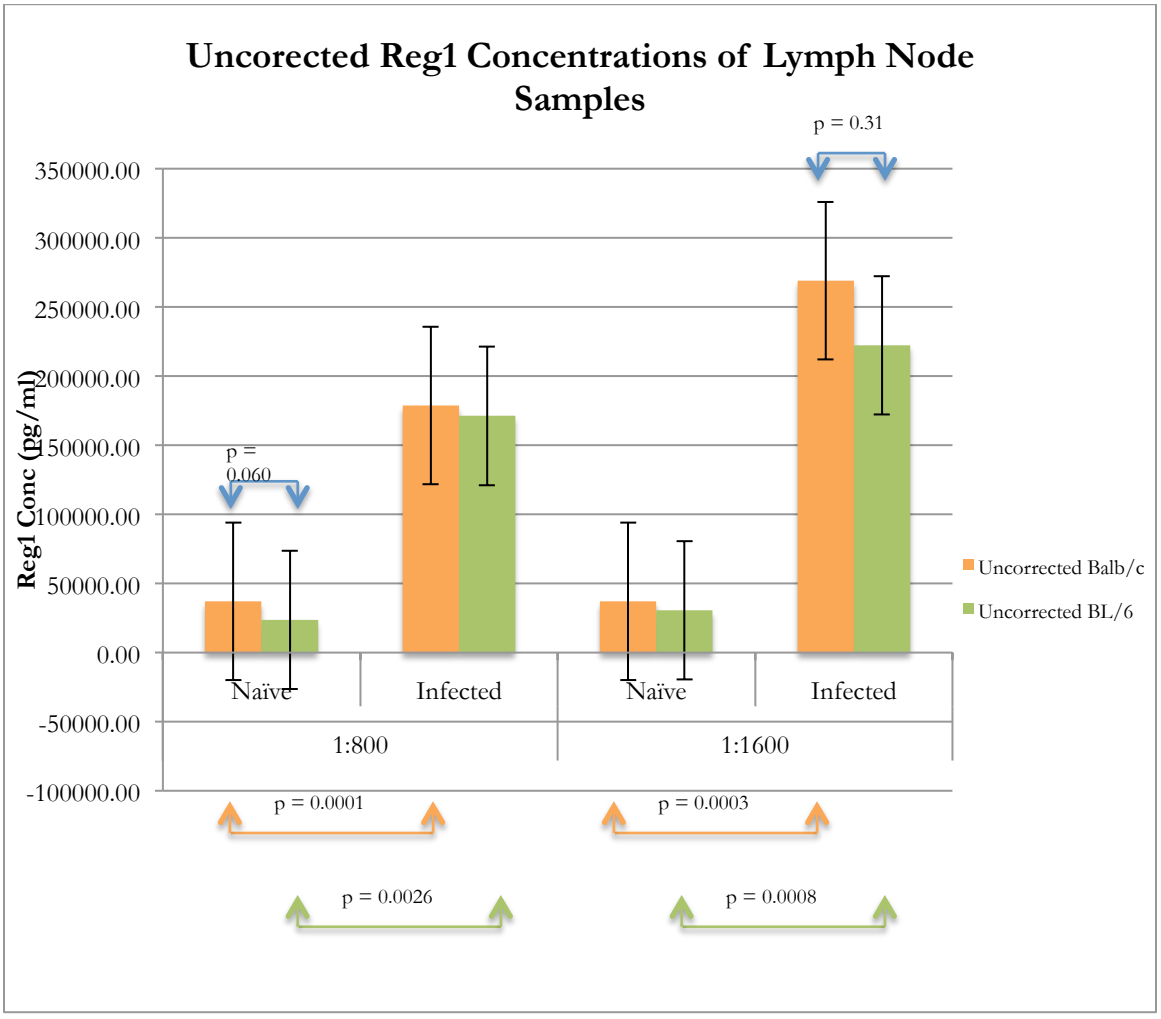

Figure 19. Bar graph comparing the means of uncorrected Reg1 concentration in mouse peripheral lymph node tissue samples in each group.

Infected samples diluted at 1:800 seemed to have 9 times as more Reg1 protein than the naïve samples at the same dilution. Infected samples diluted 1:1600 had a larger difference in Reg1 concentration, as they seemed to have about 10 times as much Reg1 as naïve samples of the same dilution. In both dilutions, naïve BALB/c seems to be making more than naïve BL/6, and infected BALB/c seems to be making more than infected BL/6. However, the high p values comparing these two groups indicate that the difference is not statistically significant.

Like with the spleen samples, the Bradford assay was also used to correct the lymph node Reg1 concentration data. Figure 20 shows a bar chart that compares the mean Bradford Corrected Reg1 concentrations of the two strains of mice against each other, at each health condition and at each sample dilution factor. For samples diluted at 1:800, the mean Bradford Corrected Reg1 concentration of lymph node tissue in the BALB/c naïve group was about 60pg/ug, and 45pg/ug in the BL/6 naïve group. Infected tissue samples had about a 3-fold increase in Reg1 concentration compared to the naïve tissue samples. The mean Bradford Corrected Reg1 concentration of lymph node tissue in the infected BALB/c group was about 160pg/ug, and about 210pg/ug in the infected BL/6 group.

For samples diluted at 1:1600, the mean Bradford Corrected Reg1 concentration of lymph node tissue in the BALB/c naïve group was about 55pg/ug, and about 60pg/ug in the BL/6 naïve group. Bradford Corrected Reg1 concentration in infected tissue samples increased by almost 4-fold at the same dilution. The mean Bradford Corrected Reg1 concentration of lymph node tissue in the infected BALB/c group was about 230pg/ug while the infected BL/6 group had a mean of about 260pg/ug.

The p values of the *t*-tests comparing different sample groups are summarized in Table 3. Of the groups compared, only the comparisons between naïve and infected samples within the same strains yielded p values lower than 0.05. Therefore the difference in Reg1 concentration between strains at each health condition was not statistically significant. However, in both strains, the difference in Reg1 concentration from naïve to infected conditions was statistically significant indicating that infection lead to a significant change in the concentration of Reg1 in these samples.

Table 3. P values resulting from the comparison of Bradford corrected Reg1 concentration values of different sample groups of lymph node tissue

Dilution	Group Comparisons	P values
1:800	Naïve BALB/c and Naïve BL/6	0.28
	Infected B BALB/c and Infected BL/6	0.52
	Naïve BALB/c and Infected BALB/c	0.031
	Naïve BL/6 and Infected BL/6	0.042
1:1600	Naïve BALB/c and Naïve BL/6	0.81
	Infected B BALB/c and Infected BL/6	0.60
	Naïve BALB/c and Infected BALB/c	0.0043
	Naïve BL/6 and Infected BL/6	0.0024

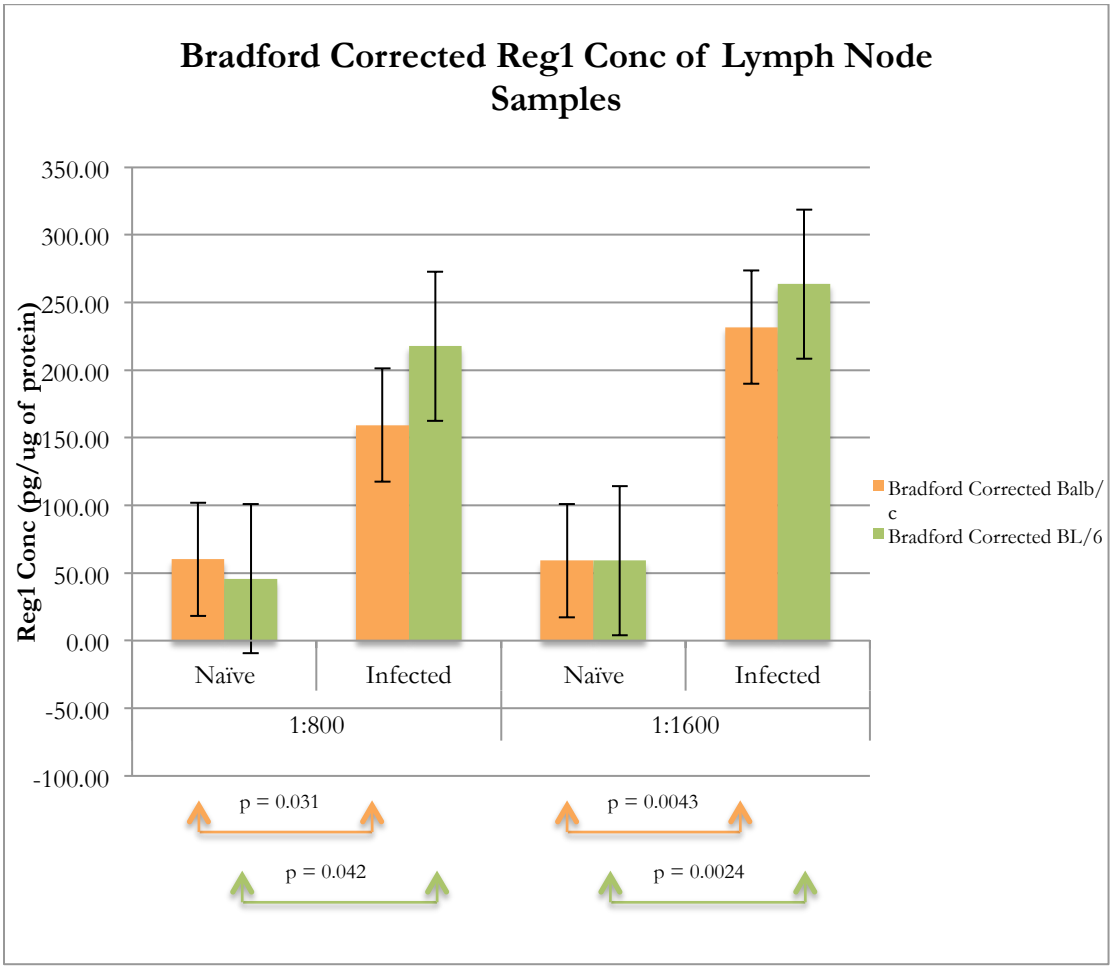

Figure 20. Bar graph comparing the means of Bradford Corrected Reg1 concentration in mouse lymph node tissue samples in each group.

Infected samples diluted at 1:800 seemed to have 3 times as more Reg1 protein than the naïve samples at the same dilution. Infected samples diluted 1:1600 had a larger difference in Reg1 concentration, as they seemed to have about 4 times as much Reg1 as naïve samples of the same dilution. In both dilutions, naïve BALB/c seems to be making more than naïve BL/6, and infected BL/6 seems to be making more than infected BALB/c. However, the high p values gotten when comparing these two groups indicate that the difference between them is not statistically significant.

Results of the ANOVA analysis on the lymph node samples are shown in Figures 21 and 22. When comparing the Log of Bradford Corrected Reg1 concentration levels of samples diluted 1:800 between mouse strains before infection, the two strains of mice have comparable levels of Reg1 in their lymph nodes (Figure 21). In the same vein, the concentration of Reg1 protein in both mouse strains 3.5 days post infection are also comparable. It should be noted that BALB/c mice seem to be making slightly more Reg1 than BL/6 mice at the naïve state, and BL/6 slightly more than BALB/c at the infected state. However, the p value ($p = 0.998$) gotten from the ANOVA analysis indicates that the difference between strains at each health condition is not statistically significant. When comparing the Reg1 concentration in lymph node samples across health conditions, both mouse strains have more Bradford Corrected Reg1 when infected than they do uninfected. The p value ($p = 0.0001$) gotten from the ANOVA analysis confirms that the health condition (naïve or infected) has a significant effect on the concentration of Reg1 in mouse lymph node samples. Therefore, the results of the ANOVA confirm the results of previously conducted group *t*-tests. The ANOVA analysis also tested for interaction between the two factors, and the p value of 0.281 indicates that there is no statistical interaction.

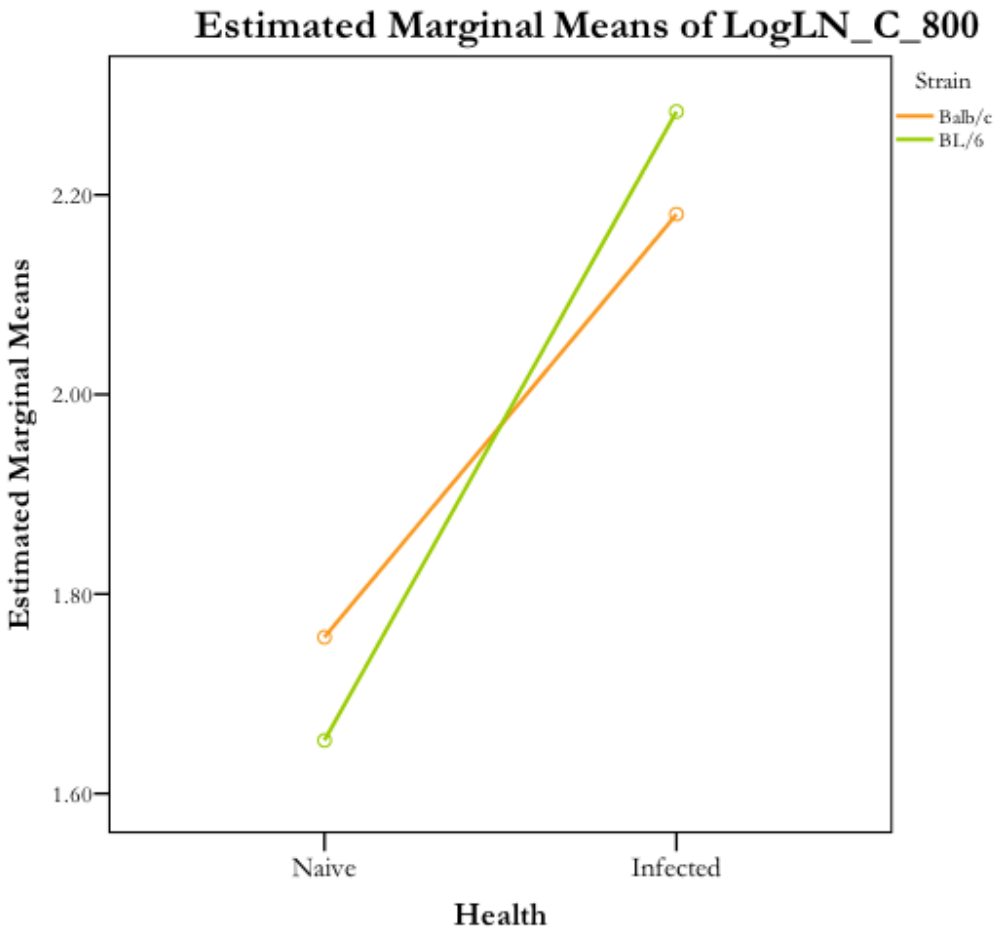

Figure 21. Interaction graph showing how the two factors (health condition and strain) affect the response (Log of Bradford Corrected Reg1 concentration) of lymph node samples diluted at 1:800.

Bradford Corrected Reg1 concentration in lymph node samples increases from naïve to infected for both animal strains. However, this there is no significant difference between the two mouse strains at each health condition.

For lymph node samples diluted 1:1600, the Log of Bradford Corrected Reg1 was higher in the BL/6 strain at both health conditions. However, this difference in strain at each health condition also was deemed to be insignificant by the p value ($p = 0.57$). On the other hand the difference in health conditions had a significant effect ($p = 0.0001$) on the presence of Reg1 in these samples. There was no interaction to be found between these two factors ($p = 0.916$).

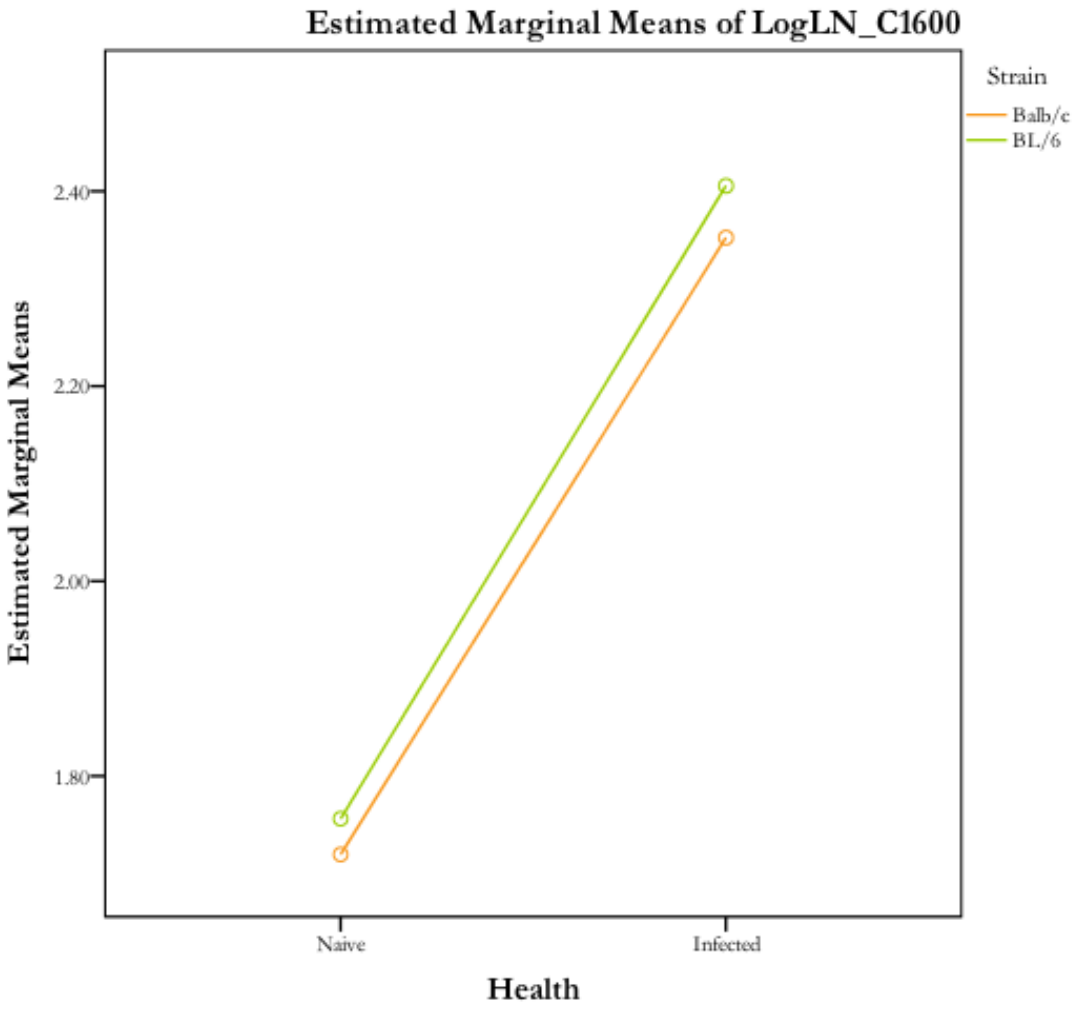

Figure 22. Interaction graph showing how the two factors (health condition and strain) affect the response (Log of Bradford Corrected Reg1 concentration) of lymph node samples diluted at 1:1600.

Bradford Corrected Reg1 concentration in lymph node samples increases from naïve to infected for both animal strains. However, this there is no significant difference between the two mouse strains at each health condition.

Mesenteric Lymph Node

Reg1 concentration data collected from the mesenteric lymph nodes was treated in the same way as data collected from the spleen and other lymph nodes. Figure 23 shows the means of uncorrected Reg1 mouse samples per group in a bar chart. This bar chart compares the mean Reg1 concentrations of two strains of mice against each other at each health condition, and at each sample dilution factor. For samples diluted at 1:800, the mean concentration of Reg1 in mesenteric lymph node tissue of the BALB/c naïve group was about 27,000pg/mL, and about 17,000pg/mL in BL/6. Infected tissue samples at the same dilution had about a 6-fold increase in Reg1 concentration than the naïve tissue samples. The mean Reg1 concentration of 1:800 diluted mesenteric lymph node samples in the infected BALB/c group was about 170,000pg/mL and, about 130,000pg/mL in BL/6.

For samples diluted at 1:1600, mean concentration of Reg1 in mesenteric lymph node tissue of the BALB/c naïve group was about 37,000pg/mL, and about 20,000pg/mL in the BL/6 naïve group. Infected tissue samples increased almost by a 10-fold in Reg1 concentration compared to the naïve tissues at the same dilution. The mean concentration of Reg1 in mesenteric lymph node tissue of the infected BALB/c group was about 270,000pg/mL, and about 175,000pg/mL in the BL/6 group.

The p values resulting from the comparison between different sample groups is summarized in Table 4. Of the groups compared, only the comparisons between naïve and infected samples within the same strains yielded p values lower than 0.05. Therefore the difference in Reg1 concentration between strains at each health condition was not statistically significant. However, in both strains, the difference in Reg1 concentration from naïve to infected conditions was statistically significant indicating that infection lead to a significant change in the concentration of Reg1 in these samples.

Table 4. P values resulting from the comparison of uncorrected Reg1 concentration values of different sample groups of mesenteric lymph node tissue.

Dilution	Group Comparisons	P values
1:800	Naïve BALB/c and Naïve BL/6	0.35
	Infected B BALB/c and Infected BL/6	0.43
	Naïve BALB/c and Infected BALB/c	0.0059
	Naïve BL/6 and Infected BL/6	0.015
1:1600	Naïve BALB/c and Naïve BL/6	0.24
	Infected B BALB/c and Infected BL/6	0.44
	Naïve BALB/c and Infected BALB/c	0.068
	Naïve BL/6 and Infected BL/6	0.014

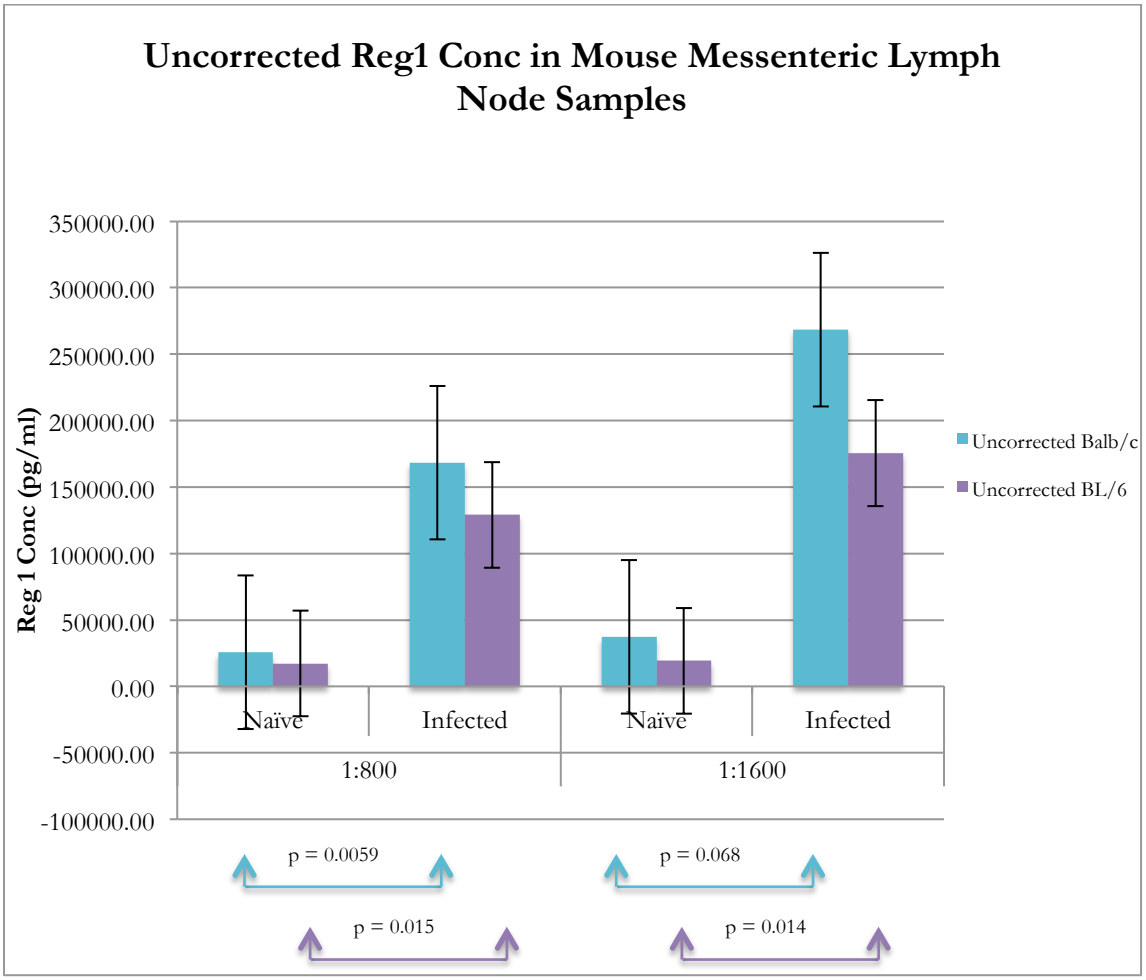

Figure 23. Bar graph comparing the means of Uncorrected Reg1 concentration in mouse mesenteric lymph node tissue samples in each group.

Infected samples diluted at 1:800 seemed to have 6 times as more Reg1 protein than the naïve samples at the same dilution. Infected samples diluted 1:1600 had a larger difference in Reg1 concentration, as they seemed to have about 10 times as much Reg1 as naïve samples of the same dilution. In both dilutions, naïve BALB/c seems to be making more than naïve BL/6, and infected BALB/c seems to be making more than infected BL/6. However, the high p values gotten when comparing these two groups indicate that the difference between them is not statistically significant.

As it was done for the other secondary lymphoid tissue samples, the Bradford assay was also used to correct the mesenteric lymph node Reg1 concentration data. Figure 24 shows a bar chart that compares the mean Bradford Corrected Reg1 concentrations of the two strains of mice against each other, at each health condition and at each sample dilution factor. For samples diluted at 1:800, the mean Bradford Corrected Reg1 concentration of mesenteric lymph node tissue in the BALB/c naïve group was about 38pg/ug, and 20pg/ug in the BL/6 naïve group. Infected tissue samples had about a 3-fold increase in Reg1 concentration compared to the naïve tissue samples. The mean Bradford Corrected Reg1 concentration of mesenteric lymph node tissue in the infected BALB/c group was about 110pg/ug, and about 74pg/ug in the infected BL/6 group.

For samples diluted at 1:1600, the mean Bradford Corrected Reg1 concentration of mesenteric lymph node tissue in the BALB/c naïve group was about 49pg/ug, while it was about 25pg/ug in the BL/6 naïve group. Bradford Corrected Reg1 concentration in infected tissue samples at this dilution increased by almost 4-fold. The mean Bradford Corrected Reg1 concentration of mesenteric lymph node tissue in the infected BALB/c group was about 160pg/ug while the infected BL/6 group had a mean Bradford Corrected Reg1 concentration of about 99pg/ug.

Table 5 summarizes the p values obtained from the *t*-test comparison between different sample groups. In samples diluted 1:800, all the comparisons between the groups listed in Table 5 have p values less than 0.05 indicating statistical significance. Therefore the difference in Reg1 expression between naïve groups of both strains, and naïve and infected groups of each strain are statistically significant. This indicates that, in addition to the health condition (infected or naïve) of the mice having a statistically significant influence of the amount of Reg1 present in their mesenteric lymph nodes, the type of mouse strain they belong to also has statistically significant influence on the concentration of Reg1 in this tissue.

Table 5. P values resulting from the comparison of Bradford corrected Reg1 concentration values of different sample groups of mesenteric lymph node tissue

Dilution	Group Comparisons	P values
1:800	Naïve BALB/c and Naïve BL/6	0.0075
	Infected B BALB/c and Infected BL/6	0.046
	Naïve BALB/c and Infected BALB/c	0.0017
	Naïve BL/6 and Infected BL/6	0.0023
1:1600	Naïve BALB/c and Naïve BL/6	0.56
	Infected B BALB/c and Infected BL/6	0.22
	Naïve BALB/c and Infected BALB/c	0.086
	Naïve BL/6 and Infected BL/6	0.0008

On the other hand, the *t*-test results of samples dilutes 1:1600 reflected those of the spleen and peripheral lymph nodes. Of the groups compared, only the comparisons between naïve and infected samples within the BL/6 strain yielded a p value lower than 0.05. The difference in Reg1 concentration of the BL/6 strain from naïve to infected conditions was statistically significant

indicating that infection lead to a significant change in the concentration of Reg1 in these samples. Conversely, the difference in Reg1 concentration between strains at each health condition was not statistically significant, neither was the difference in Reg1 concentration within the BALB/c strain at both health conditions. This indicates that the effect of health condition on Reg1 concentration within the BALB/c strain was not statistically significant, and neither was the effect of mouse strain type on Reg1 concentration at each health condition.

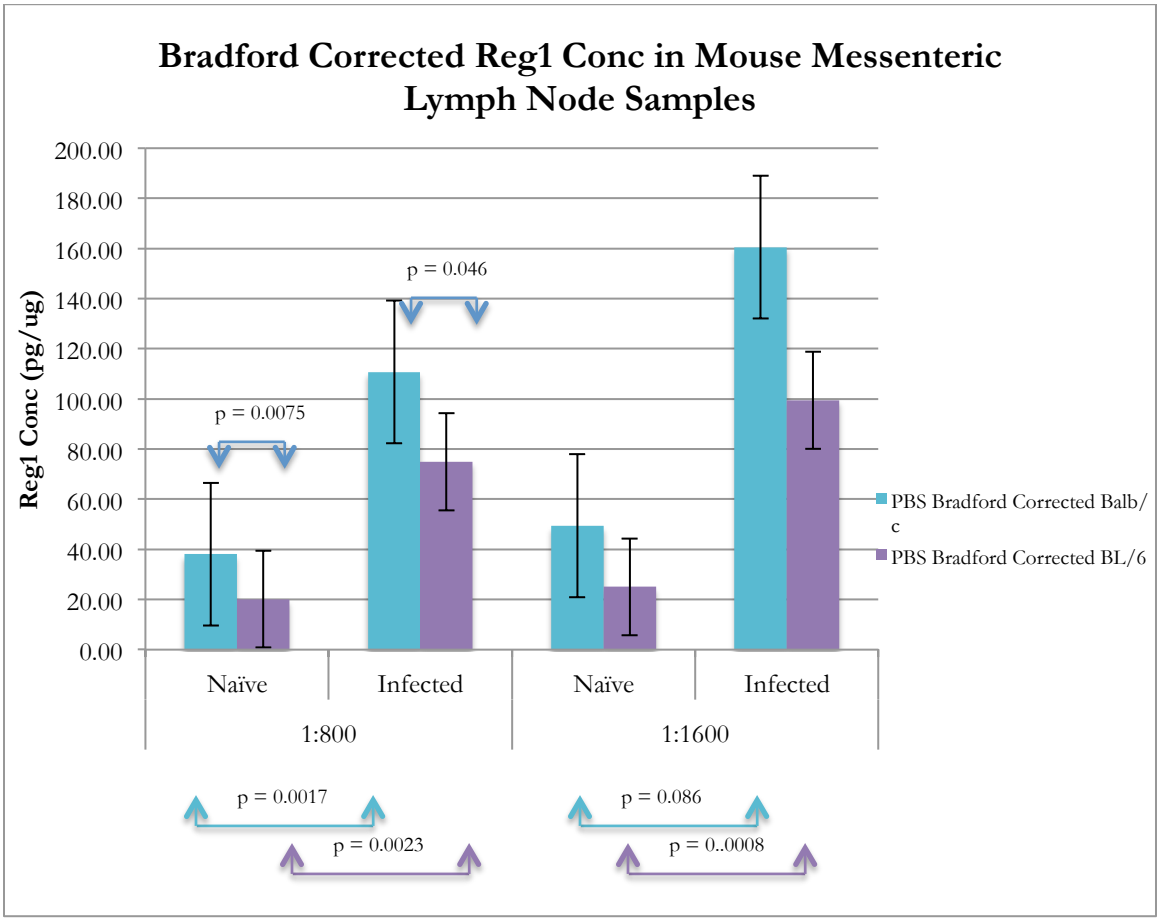

Figure 24. Bar graph comparing the means of Bradford Corrected Reg1 concentration in mouse mesenteric lymph node tissue samples in each group.

Infected samples diluted at 1:800 seemed to have 3 times as more Reg1 protein than the naïve samples at the same dilution. Infected samples diluted 1:1600 had a larger difference in Reg1 concentration, as they seemed to have about 4 times as much Reg1 as naïve samples of the same dilution. In both dilutions, naïve BALB/c seems to be making more than naïve BL/6, and infected BALB/c seems to be making more than infected BL/6. The p values gotten when comparing the 1:800 diluted samples of both strains at naïve and infected time points indicate that the difference in Reg1 concentration between BALB/c and BL/6 is statistically significant. On the other had, the p values gotten when comparing 1:1600 diluted samples of both strains indicates that the difference in Reg1 concentration between BALB/c and BL/6 is not statistically significant.

Results of the ANOVA analysis on the mesenteric lymph node samples are shown in Figures 25 and 26. When comparing the Log of Bradford Corrected Reg1 concentration levels of samples diluted 1:800 across mouse strains before infection, the two strains of mice have comparable levels of Reg1 in their lymph nodes (Figure 25). In the same vein, the concentration of Reg1 protein in both mouse strains 3.5 days post infection are also comparable. It should be noted that BALB/c mice seem to be making slightly more Reg1 than BL/6 mice at both naïve and infected states. Therefore, the strain type has a statistically significant effect on the concentration of Reg1 in mouse mesenteric lymph node samples.

The p value ($p = 0.001$) gotten from the ANOVA analysis indicates that the difference in Reg1 concentration between both strains at each health condition is statistically significant. When comparing the Reg1 concentration in mesenteric lymph node samples across health conditions, both mouse strains have more Bradford Corrected Reg1 when infected than they do uninfected. The p value ($p = 0.00001$) gotten from the ANOVA analysis confirms that the health condition (naïve or infected) has a significant effect on the concentration of Reg1 in mouse mesenteric lymph node samples. Therefore, the results of the ANOVA confirm the results of previously conducted group *t*-tests. The ANOVA analysis also tested for interaction between the two factors, and the p value of 0.316 indicates that there is no interaction.

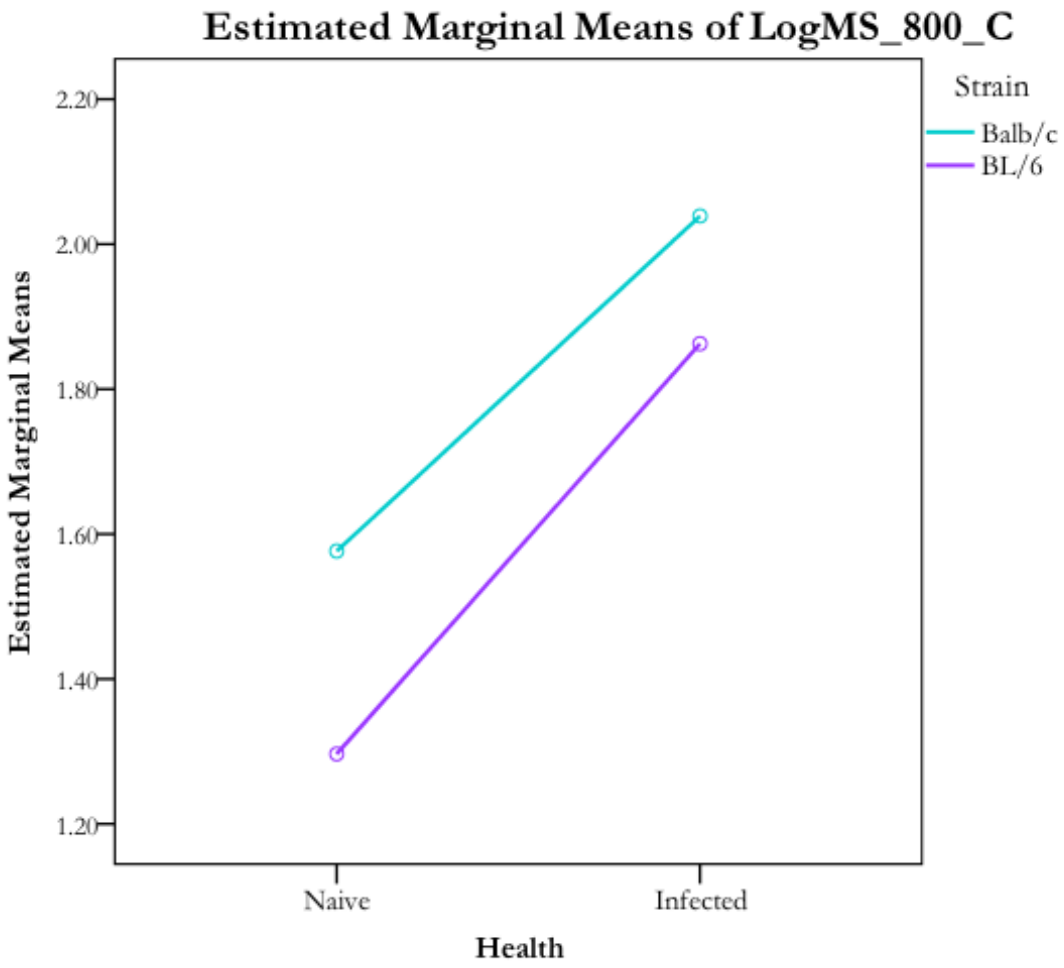

Figure 25. Interaction graph showing how the two factors (health condition and strain) affect the response (Log of Bradford Corrected Reg1 concentration) of mesenteric lymph node samples diluted at 1:800.

Bradford Corrected Reg1 concentration in mesenteric lymph node samples increases from naïve to infected for both animal strains. In addition to this, there is a statistically significant difference between the Reg1 concentrations of the two mouse strains at each health condition.

The ANOVA analysis of Bradford corrected Reg1 concentration in mesenteric lymph nodes samples diluted 1:1600 gave a slightly different interpretation. Although concentration of Reg1 seemed to be higher in BALB/c than BL/6 at both naïve and infected states, this difference due to strain was deemed insignificant by the p value ($p = 0.040$). This was because we set a conservative threshold for ANOVA significance at ($p = 0.03$). On the other hand, difference in health conditions had a significant effect ($p = 0.0001$) on the presence of Reg1 in these samples, indicating that health condition has a significant effect on the concentration of Reg1 in mouse mesenteric lymph node samples. Lastly, there was no interaction found between the two factors, strain and health condition ($p = 0.916$).

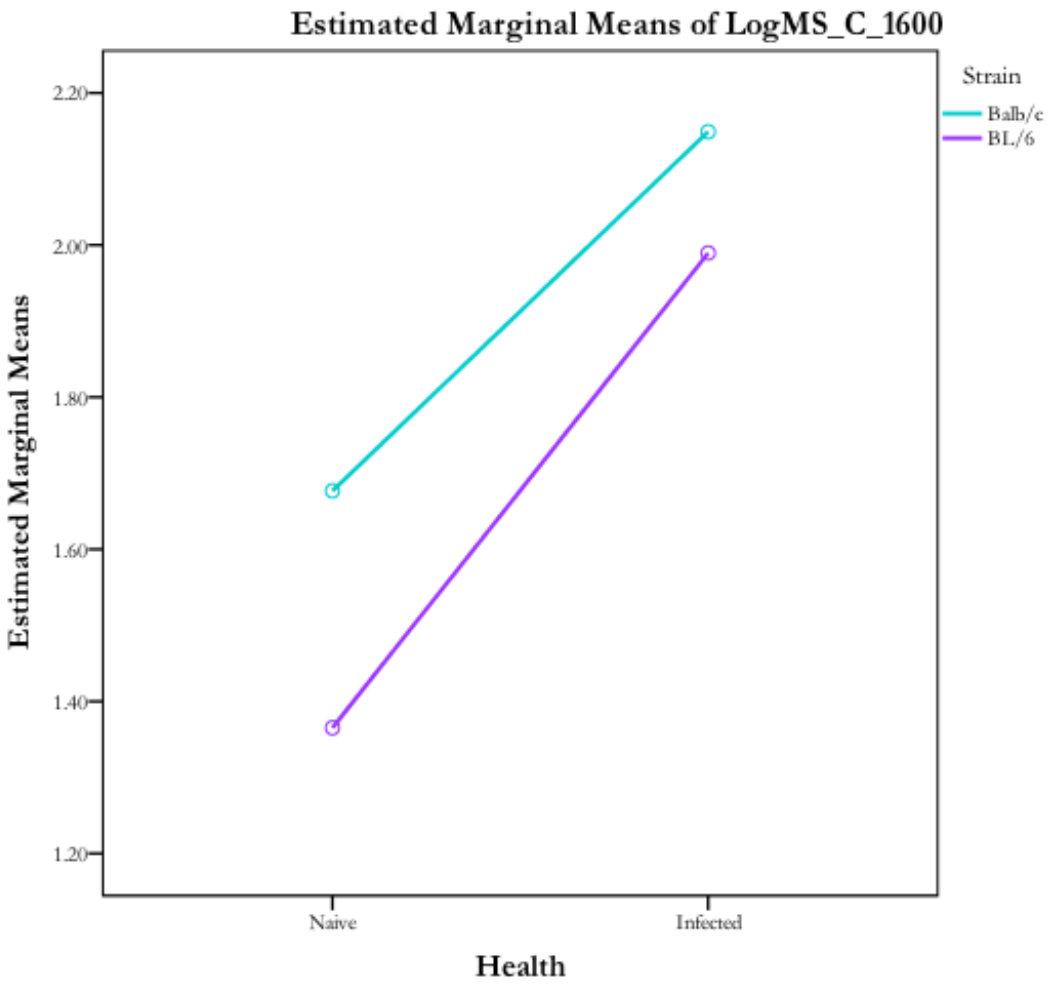

Figure 26. Interaction graph showing how the two factors (health condition and strain) affect the response (Log of Bradford Corrected Reg1 concentration) of mesenteric lymph node samples diluted at 1:1600.

Bradford Corrected Reg1 concentration in lymph node samples increases from naïve to infected for both animal strains. However, this there is no statistically significant difference between the two mouse strains at each health

DISCUSSION

Proteins in the mammalian body are constantly being degraded and replaced by new synthesis (Goldberg and St. John, 1976). The degradation of proteins by mammalian cells can occur in a number of ways, some of which include the degradation of phagocytized extracellular proteins by the lysosome, and the degradation of intracellular proteins by the proteasome (Rock and Goldberg, 1999).

Proteases are enzymes that control biological processes by catalyzing the precisely timed, rapid turnover of key regulatory proteins (Maupin-Furlow *et al.*, 2009). In addition to catalyzing regulatory proteins, proteases are involved in the immune system and take up various forms, one of which is the proteasome. The proteasome is a large nuclear protease complex that is responsible for the majority of non-lysosomal protein degradation within eukaryotic cells (Ferrer *et al.*, 2004). As described in the introduction, intercellular proteins degraded by proteasomes in antigen presenting cells are presented via MHC Class I (Figure 4) to cytotoxic T cells.

For effective protein degradation, proteasomes work together with the regulatory protein ubiquitin. Ubiquitin tags antigenic peptides for degradation and directs them to the 26S proteasome complex. The proteolytic part of the 26S

complex is the 20S core particle, a cylindrical structure made up of four stacked rings (Baumeister *et al.*, 1998; Coux *et al.*, 1996). The two central rings contain the proteolytic active sites, and are made up of homologous but distinct ß-subunits. The rings at the ends of the cylinder are made up of different but homologous α-subunits, and have smaller diameters compared to those of the two middle rings (Rock and Goldberg, 1999). This organization of the 20S core particle restricts substrate entry and allows efficient degradation of proteins transported to the proteasome, while protecting the other cell components from nonspecific proteolytic attack (Rock and Goldberg, 1999).

The immunoproteasome is a specific kind of proteasome isoform induced by interferons (Krüger and Kloetzel, 2012), proteins that derive their name from their ability to interfere with viral growth (Commins *et al.*, 2010). In response to an encounter with pathogens, some cells of the immune response such as macrophages, secrete interferons (Kontsek and Kontsekova, 1997), which go on to trigger the protective defenses of the immune system that eradicate the pathogen. When exposed to interferon-γ (IFN-γ) in mammalian cells (Baumeister *et al.*, 1998), the homologous ß-subunits of the 20S core particle are replaced by other catalytic subunits (LMP2, LMP7 and MECL-1) and proteasomes become immunoproteasomes (Kloetzel, 2001; Tanaka and Kasahara, 1998). The catalytic sites of the immunoproteasome are thus different from that of the regular proteasome. These new catalytic sites are characterized by increases in

chymotrypsin- and trypsin-like activities attributed to serine proteases. These activities enhance the proteasome's capacity to generate antigenic epitopes that fit better in MHC Class I molecules (Kloetzel, 2001; Rock *et al.*, 2002; Tanaka and Kasahara, 1998).

The importance of the immunoproteasome has been established in several experiments. Van Kaer *et al.* (1992, 1994) discovered that LMP2-deficient mice were defective in presenting some viral antigens such as influenza nucleoprotein, via MHC Class I. A similar experiment by Fehling *et al.* (1994) revealed that LMP7 deficient mice had less MHC Class I cell surface expression. These results indicate that antigen presentation may also be affected by serine proteases that make up the immunoproteasome.

Regular proteasomes and immunoproteasomes usually coexist in mammalian cells but the ratio between the two isoforms depends on the type of cell and tissue, and the environmental condition (Noda *et al.*, 2000). Dendritic cells have been identified as one of the antigen presenting cells that exclusively express immunoproteasomes. Although immature dendritic cells express an equal number of proteasomes and immunoproteasomes (Van den Eynde and Morel, 2001), dendritic cells that have been induced to mature contain only immunoproteasomes (Macagno *et al.*, 1999). As mentioned earlier in the introduction, dendritic cells are the strongest antigen presenting cells due to their

ability to present antigens via MHC Class I and Class II. Thus they influence the actions of both CD4+ and CD8+ T cells. Research by Palmowski *et al.* (2006) reveals that the presence of immunoproteasomes is also instrumental in the ability of dendritic cells to present antigenic peptides via MHC Class II. Dendritic cells are also important in T cell development as they negatively select self-antigen binding T cells for elimination (Parham, 2009). Thus in addition to determining how antigenic peptides are presented, immunoproteasomes present in dendritic cells also possibly play a part in the level of the repertoire of CD8+ T cells available for antiviral responses. Therefore, with the expression of immunoproteasome-dependent epitopes, certain pathogens may be able to evade destruction in immunoproteasome deficient animals.

The process of ridding the body of pathogens can have adverse effects on uninfected cells that may be caught in the crossfire. Inflammation and interferon signaling may confer stress to uninfected cells in the form of radicals, resulting in oxidant-damaged proteins (Krüger and Kloetzel, 2012). Therefore in addition influencing T cell activity, the immunoproteasome maintain immune homeostasis by preserving cell viability and tissue integrity. The immunoproteasome does this by degrading oxidant-damaged protein and thus preventing the build up of potentially toxic protein aggregates. Certain neurodegenerative diseases, such as Alzheimer and Huntington's diseases, have been characterized by the deposition of abnormal proteins in the cytoplasm and nuclei of nerve cells (Sherman and

Goldberg, 2001), and recent research has implicated proteasomes and immunoproteasomes in the pathophysiology of these diseases (de Vrij *et al.*, 2004; Mishto, *et al.*, 2006; Díaz-Hernández *et al.*, 2003).

Since its development, the MAIDS model has been instrumental in understanding the pathology of AIDS. The study of the immunoproteasome and the proteases that comprise it, in the context of the MAIDS model, may help us uncover pathways that could lead to the elimination of HIV in humans. The Stranford lab has established that some genes that lead to the production of certain serine proteases products found in the immunoproteasome, are differentially expressed in MAIDS resistant and susceptible mouse strains (Tepsuporn *et al.*, 2008). The aim of this thesis was to quantify one of such serine proteases, the regenerating islet-derived I protein, in both mouse strains and determine whether or not it contributes to MAIDS susceptibility.

Reg1 protein expression in Mesenteric Lymph Nodes differs in BALB/c and C57BL/6 mice

An indirect ELISA was designed to measure the amount of Reg1 protein in spleen, lymph node and mesenteric lymph node of BALB/c resistant and BL/6 susceptible mice. The evaluation of the result of this experiment revealed

that Reg1 concentration in all tissues tested increased from naïve to infected states in both animal strains. However, only the results obtained from the mesenteric lymph node showed a statistical difference between the Reg1 concentration of BALB/c and BL/6 mice at both naïve and infected conditions. The naïve BALB/c resistant strain made statistically significant more Reg1 than the naïve BL/6 susceptible strain. Similarly, infected BALB/c animals made more Reg1 than infected BL/6 animals. These protein quantification results are not in accordance with Tepsuporn *et al.*'s (2008) DNA microarray results, which show that the Reg1 gene is more differentially expressed in the lymph node and spleen of BALB/c than those of BL/6 three days post infection. This discrepancy between the DNA data and the protein concentration data is evidence for how the presence of DNA does not always translate into the presence of a protein product.

A possible explanation for the inconsistency in the amount of Reg1 produced by secondary lymphoid organs is that mesenteric lymph nodes behave slightly differently from the other lymph nodes. Scattered around the small intestine, the mesenteric lymph nodes are the draining lymph nodes for infections that get into the body via the gastrointestinal tract, and by extension, other mucosal surfaces. Thus the immune cells that circulate around the mesenteric lymph nodes and other mucosal surface lymph nodes are slightly different from their peripheral counterparts. The gastrointestinal tract also contains most of the

secondary lymphoid tissue in the body; hence the mesenteric lymph node contains more immune cells than the peripheral lymph nodes (MacDonald and Spencer, 1994). Therefore a larger number of immune cells in the mesenteric lymph nodes should result in a corresponding higher number of their associated proteins, including serine proteases.

Furthermore, the MuLV virus was introduced into the body via an intraperitoneal injection. Since the mesenteric lymph nodes are the draining lymph nodes of the intraperitoneal region, the immune response will most likely start there and may take a few days to get to the peripheral lymph nodes. Therefore, testing for Reg1 concentration a few more days post MuLV infection may result in more homogenous results in all secondary lymphoid organs.

The higher concentration of Reg1 in both naïve and infected BALB/c resistant compared to both categories of the BL/6 susceptible strain has many implications. These implications include: i) BALB/c mice have a larger ratio of immunoproteasome to regular proteasome, thus making their APCs (dendritic cells) more effective at presenting antigens to the T cells; ii) that BL/6 mice have defective immunoproteasomes (problematic catalytic sites) that are not as effective in presenting antigenic peptides via MHC Class I, as healthy immunoproteasomes; iii) impaired expression of genes that affect the production of serine proteases and immunoproteasome. Earlier scientific studies have

confirmed that the catalytic sites in immunoproteasomes are characterized by serine proteases, and the presence of immunoproteasomes make for a more effective antigen presenting dendritic cell. Improved MHC Class I presentation by dendritic cells will result in the better detection of antigen by T cells and this would lead to a more effective eradication of infection.

Antigen presenting cells' ability to organize an appropriate immune response is largely influenced by external cues such as cytokines and chemokines. The presence of IFN-γ in mammalian cells affects the transition from ordinary proteasome to immunoproteasome. Thus, a lower concentration of IFN-γ in BL/c may have resulted in little or no immunoproteasomes present in its immune cells. On the other hand, a high concentration of IFN-γ in BALB/c may have lead to a high number of immunoproteasomes, and result in a high concentration of serine proteases, Reg1 included.

Sources of Error

The experimental procedure for this study involved several hour-long steps as out lined in the Materials and Methods section. As a result, the tendency for error was present although it was avoided as best as possible.

The first possible source of experimental error lies in the infection of the mice. It is possible that some amount of virus remained in the syringe after the infection of some mice and thus, some mice received less than the designated viral titer. A lower viral titer may have influenced the timing and course of the infection.

A second source of error may have occurred during the isolation and homogenization of the secondary lymphoid organs. Although the spleen is a relatively large and easily identifiable organ, the lymph nodes are smaller and harder to distinguish from the fat they are in close proximity with. There were sometimes during the experiment when isolated lymph nodes turned out to be globs of fat. Unlike the spleen, which is relatively easy to homogenize, the lymph nodes are small and harder to homogenize. Often times, the lymph nodes had to be dislodged from the tip of the homogenizer. The possible loss of lymph nodes during homogenization and the presence of fat instead of lymph node tissue may have resulted in smaller lymph node sample sizes and thus less protein. This possible reduction in lymph node sample sizes may have contributed to the experimental errors.

Future Studies

This research project managed to answer the question of whether or not the differential gene expression of Reg1 in BALB/c versus BL/6 as observed by Tepsuporn *et al.*, (2008), translated to a protein difference. However, this study has given rise to a number of questions we would like to answer to better understand the role of Reg1 in the MAIDS model. Before initiating experiments to answer these questions, we propose that this experiment be repeated with a larger number of animals. The number of animals present in each group of this study was n = 4. Increasing this number would reduce variability within a group and result in more obvious trends in Reg1 expression.

To confirm if mesenteric lymph nodes respond differently to the intraperitoneally introduced infection than the peripheral lymph nodes do, we propose that viral expression in each sample be measured and compared to the concentration of Reg1 protein present in the sample.

Since the role of Reg1 protein in the immune system is still being speculated, it would be helpful to figure out which immune cells are producing it. To do so we propose that dendritic cells, which are known to have higher immunoproteasome levels than other immune cells, be isolated from the

secondary lymphoid organ samples and tested for Reg1. The samples without dendritic cells should also be tested and used for comparison.

In addition to this, we propose that the Reg1 gene in both BALB/c and BL/6 be knocked out, and the experimental procedure described in this paper be carried out on them. From this procedure we hope to see if the knockout mice react to the virus differently, and thus we hope to gain a clearer picture of the role of Reg1 in the MAIDS model.

We also propose that the protein product of all the resistance-associated genes identified by Tepsuporn *et al.*, (2008) be identified and quantified in animals of the MAIDS model.

Lastly, we propose that the connection between IFN-γ and serine proteases be explored. Does a low IFN-γ concentration translate to a lower serine protease (Reg1) concentration?

Further investigation into the sources of Reg1 protein, the consequences of its absence, and its interaction with other serine proteases that are identified as resistance-associated genes, may provide insight into the pathology of MuLV/MAIDS and by extension, HIV/AIDS.

REFERENCES

Adkison, A. M., S. Z. Raptis, D. G. Kelley, and C. T. N. Pham. 2002. Dipeptidyl peptidase I activates neutrophil-derived serine proteases and regulates the development of acute experimental arthritis. *Journal of Clinical Investigation* 109: 363-371.

Aggleton, P., E. Yankah, M. Crewe, D. P. Baker, J. Leon, and J. M. Collins. 2011. Education and HIV/AIDS-30 Years on. *Aids and Behavior* 23; 15: 495; 1319-507; 1327.

Aimes, R. T., A. Zijlstra, J. D. Hooper, S. M. Ogbourne, M. L. Sit, S. Fuchs, D. C. Gotley, J. P. Quigley, and T. M. Antalis. 2003. Endothelial cell serine proteases expressed during vascular morphogenesis and angiogenesis. *Journal of Thrombosis and Haemostasis* 89: 561-572.

Akalu, Y. 2012. Early Differential IDO Expression Patterns In The MAIDS Model [electronic resource] / Yemsratch Akalu. Honors Thesis, Mount Holyoke College.

Akira, S., S. Uematsu, and O. Takeuchi. Review: Pathogen Recognition and Innate Immunity. *Cell* 124: 783-801.

Aldrovandi, G. M., G. Feuer, L. Gao, B. Jamieson, M. Kristeva, I. S. Chen, and J. A. Zack. 1993. The SCID-hu mouse as a model for HIV-1 infection. *Nature* 363: 732-736.

Almonte, A. G. and J. David Sweatt. Review: Serine proteases, serine protease inhibitors, and protease-activated receptors: Roles in synaptic function and behavior. *Brain Research* 1407: 107-122.

Atlan, H. and I. R. Cohen. 1998. Immune information, self-organization and meaning. *International Immunology* 10: 711-717.

Baker, D. P., J. Leon, and J. M. Collins. 2011. Facts, Attitudes, and Health Reasoning About HIV and AIDS: Explaining the Education Effect on Condom Use Among Adults in Sub-Saharan Africa. *Aids and Behavior* 15: 1319-1327.

Baumeister, W., J. Walz, F. Zühl, and E. Seemüller. 1998. The proteasome: paradigm of a self-compartmentalizing protease. *Cell* 92: 367-380.

Baveja, U. K. and B. Rewari. 2004. Diagnosis and Management of HIV/AIDS: A Clinician's Perspective. BI Publications Pvt Ltd, New Delhi.

Beilharz, M. W., L. M. Sammels, A. Paun, K. Shaw, P. van Eeden, M. W. Watson, and M. L. Ashdown. 2004. Timed ablation of regulatory CD4+ T cells can prevent murine AIDS progression. *The Journal of Immunology* 172: 4917-4925.

Beutler, B. Innate immunity: an overview. *Molecular Immunology* 40: 845-859.

Blankson, J. N. Review: Effector mechanisms in HIV-1 infected elite controllers: Highly active immune responses? *Antiviral Research* 85: 295-302.

Bradford, M. M. 1976. A rapid and sensitive method for the quantitation of microgram quantities of protein utilizing the principle of protein-dye binding. *Analytical Biochemistry* 72: 248-254.

Brass, A. L., D. M. Dykxhoorn, Y. Benita, N. Yan, A. Engelman, R. J. Xavier, J. Lieberman, and S. J. Elledge. 2008. Identification of host proteins required for HIV infection through a functional genomic screen. *Science* 319: 921-926.

Browne, E. P., M. Kane, L. K. Case, C. Wang, L. Yurkovetskiy, S. Dikiy, and T. V. Golovkina. 2011. Toll-like Receptor 7 Controls the Anti-Retroviral Germinal Center Response. *Immunity* 7; 35: 1; 135-8; 145.

Campbell-Yesufu, O. and R. T. Gandhi. 2011. Update on Human Immunodeficiency Virus (HIV)-2 Infection. *Clinical Infectious Diseases* 52: 780-787.

Cardillo, G. 2013. Four parameters logistic regression - There and back again. *MATLAB Central*. Available at:

http://www.mathworks.com/matlabcentral/fileexchange/38122-four-parameters-logistic-regression-there-and-back-again. (Accessed: April, 2013)

Casabianca, A., C. Orlandi, A. Fraternale, and M. Magnani. 2003. A new one-step RT-PCR method for virus quantitation in murine AIDS. *Journal of Virological Methods* 110: 81-90.

Chattopadhyay, S. K., H. C. Morse, M. Makino, S. K. Ruscetti, and J. W. Hartley. 1989. Defective Virus is Associated with Induction of Murine Retrovirus-Induced Immunodeficiency Syndrome. *Proceedings of the National Academy of Sciences of the United States of America* 3862.

Clerc, O., M. Cavassini, J. Böni, J. Schüpbach, and P. Bürgisser. 2009. Case report: Prolonged seroconversion in an elite controller of HIV-1 infection. *Journal of Clinical Virology* 46: 371-373.

Colditz, I., R. Zwahlen, B. Dewald, and M. Baggiolini. 1989. In vivo inflammatory activity of neutrophil-activating factor, a novel chemotactic peptide derived from human monocytes. *American Journal of Pathology* 134: 755-760.

Commins, S. P., L. Borish, and J. W. Steinke. 2010. Immunologic messenger molecules: cytokines, interferons, and chemokines. *Journal of Allergy and Clinical Immunology* 125: S53-S72.

Corbett, E. L., R. W. Steketee, F. ter Kuile O., A. S. Latif, A. Kamali, and R. J. Hayes. 2002. HIV-1/AIDS and the control of other infectious diseases in Africa. *Lancet* 359: 2177-2187.

Coux, O., K. Tanaka, and A. L. Goldberg. 1996. Structure and functions of the 20S and 26S proteasomes. *Annual Review of Biochemistry* 65: 801-847.

de la Monte, ,S.M., M. Ozturk, and J. R. Wands. 1990. Enhanced expression of an exocrine pancreatic protein in Alzheimer's disease and the developing human brain. *Journal of Clinical Investigation* 86: 1004-1013.

de Vrij, F. M. S., D. F. Fischer, F. W. van Leeuwen, and E. M. Hol. 2004. Protein quality control in Alzheimer's disease by the ubiquitin proteasome system. *Progress in Neurobiology* 74: 249-270

Di Cera, E. 2009. Serine proteases. *IUBMB Life* 61: 510-515.

Díaz-Hernández, M., F. Hernández, E. Martín-Aparicio, P. Gómez-Ramos, M. A. Morán, J. G. Castaño, I. Ferrer, J. Avila, and J. J. Lucas. 2003. Neuronal Induction of the Immunoproteasome in Huntington's Disease. *Journal of Neuroscience* 23: 11653-11661.

Dieckgraefe, B. K., D. L. Crimmins, V. Landt, C. Houchen, S. Anant, R. Porche-Sorbet, and J. H. Ladenson. 2002. Expression of the Regenerating Gene Family in Inflammatory Bowel Disease Mucosa: Reg Iα Upregulation, Processing, and Antiapoptotic Activity. *Journal of Investigative Medicine* 50: 421.

Dunn, T. B. 1954. Normal and pathologic anatomy of the reticular tissue in laboratory mice, with a classification and discussion of neoplasms. *Journal of the National Cancer Institute.* 14: 1281-1433.

Fauci, A. S. and G. Pantaleo. 1996. Immunopathogenic mechanisms of HIV infection. *Annals of Internal Medicine* 124: 654.

Fehling, H. J., W. Swat, C. Laplace, R. Kühn, K. Rajewsky, U. Müller, and H. von Boehmer. 1994. MHC Class I Expression in Mice Lacking the Proteasome Subunit LMP-7.*Science* 1234.

Ferrer, I., B. Martín, J. Castaño G., J. J. Lucas, D. Moreno, and M. Olivé. 2004. Proteasomal expression, induction of immunoproteasome subunits, and local MHC class I presentation in myofibrillar myopathy and inclusion body myositis. *Journal of Neuropathology and Experimental Neurology* 63: 484-498.

Frankel, A. D. and J. A. Young. 1998. HIV-1: fifteen proteins and an RNA. *Annual Review of Biochemistry* 67: 1-25.

Fukuhara, H., Y. Kadowaki, T. Ose, A. Monowar, H. Imaoka, S. Ishihara, S. Takasawa, and Y. Kinoshita. 2010. In vivo evidence for the role of RegI in gastric regeneration: transgenic overexpression of RegI accelerates the healing of experimental gastric ulcers. *Laboratory Investigation* 90: 556-565.

Fukui, H., Y. Kinoshita, T. Maekawa, A. Okada, S. Waki, S. Hassan, H. Okamoto, and T. Chiba. 1998. Regenerating gene protein may mediate gastric mucosal proliferation induced by hypergastrinemia in rats. *Gastroenterology* 115: 1483-1493.

Fultz, P. N., H. M. McClure, R. B. Swenson, C. R. McGrath, A. Brodie, J. P. Getchell, F. C. Jensen, D. C. Anderson, J. R. Broderson, D. P. Francis, H. Kulaga, T. Folks, R. Rutledge, M. E. Truckenmiller, E. Gugel, and T. J. Kindt. 1989. Persistent infection of chimpanzees with human T-lymphotropic virus type III/lymphadenopathy-associated virus: a potential model for acquired immunodeficiency syndrome. *Journal of Virology* 58; 169: 116; 321-124; 326.

Gardner, M. B., E. E. Sparger, P. A. Luciw, J. H. Elder, J. K. Yamamoto, L. J. Lowenstine, and N. C. Pedersen. 1989. SIV infected rhesus macaques: an AIDS model for immunoprevention and immunotherapy. *Advances in Experimental Medicine & Biology* 251; 3: 279; S43-293; S49.

Gee, S. J., B. D. Hammock, and J. M. Van Emon. 1996. Environmental immunochemical analysis for detection of pesticides and other chemicals: a user's guide.

Ghayur, T., S. Banerjee, M. Hugunin, D. Butler, L. Herzog, A. Carter, L. Quintal, L. Sekut, R. Talanian, M. Paskind, W. Wong, R. Kamen, D. Tracey, and H. Allen. 1997. Caspase-1 processes IFN-gamma-inducing factor and regulates LPS-induced IFN-gamma production. *Nature* 386: 619-623.

Goldberg, A. L. and St. John A.C. 1976. Intracellular Protein Degradation in Mammalian and Bacterial Cells: Part 2. *Annual Review of Biochemistry* 45: 747.

Guma, M., L. Ronacher, R. Liu-Bryan, S. Takai, M. Karin, and M. Corr. 2009. Caspase independent activation of interleukin-1 in neutrophil-predominant inflammation. *Arthritis & Rheumatism* 60: 3642-3650.

Håkanson, R., D. Chen, K. Andersson, H. J. Monstein, C. M. Zhao, B. Ryberg, F. Sundler, and H. Mattsson. 1994. The biology and physiology of the ECL cell. *Yale Journal of Biology and Medicine* 67: 123-134.

Hunt, R. 2009. Human Immunodeficiency Virus and AIDS. *Microbiology and Immunology Online*. The University of South Carolina School of Medicine. Available at: http://pathmicro.med.sc.edu/lecture/hiv2000.htm (accessed: March, 2013).

Ik, L. T., R. S. Bryan, v. G. Gloria, J. M. Farrah, and C. M. Justin. 2012. Review: HIV-associated opportunistic infections of the CNS. *Lancet Neurology* 11: 605-617.

Jolicoeur, P. 1991. Murine Acquired-Immunodeficiency-Syndrome (Maids) - an Animal-Model to Study the Aids Pathogenesis. *FASEB Journal* 5: 2398-2405.

Kane, M., L. K. Case, C. Wang, L. Yurkovetskiy, S. Dikiy, and T. V. Golovkina. 2011. Innate Immune Sensing of Retroviral Infection via Toll-like Receptor 7 Occurs upon Viral Entry. *Immunity* 35: 135-145.

Kloetzel, P. M. 2001. Antigen processing by the proteasome. *Nature Reviews Molecular Cell Biology* 2: 179-187.

Kobayashi, S., T. Akiyama, K. Nata, M. Abe, M. Tajima, N. J. Shervani, M. Unno, S. Matsuno, H. Sasaki, S. Takasawa, H. Okamoto, A. L. Brass, D. M. Dykxhoorn, Y. Benita, N. Yan, A. Engelman, R. J. Xavier, J. Lieberman, and S. J. Elledge. 2008. Identification of a receptor for Reg (Regenerating gene) protein, a pancreatic beta-cell regeneration factor. *Journal of Biological Chemistry* 275; 319: 10723; 921-10726; 926.

Kontsek, P. and E. Kontsekova. 1997. Forty years of interferon. *Acta Virologica* 41: 349-354.

Kraut, J. 1977. Serine Proteases: Structure and Mechanism of Catalysis. *Annual Review of Biochemistry* 46: 331.

Krüger, E. and P. Kloetzel. 2012. Immunoproteasomes at the interface of innate and adaptive immune responses: two faces of one enzyme. *Current Opinion in Immunology* 24: 77-83.

Kulaga, H., T. Folks, R. Rutledge, M. E. Truckenmiller, E. Gugel, and T. J. Kindt. 1989. Infection of Rabbits with Human Immunodeficiency Virus-1 - a Small Animal-Model for Acquired Immunodeficiency Syndrome. *Journal of Experimental Medicine* 169: 321-326.

Larsen, C. G., A. O. Anderson, E. Appella, J. J. Oppenheim, and K. Matsushima. 1989. The Neutrophil-Activating Protein (NAP-1) is also Chemotactic for T Lymphocytes. *Science* 243: 1464-1466.

Levy, J. A. 1993. Pathogenesis of Human-Immunodeficiency-Virus Infection. *Microbiological Reviews* 57: 183-289.

Li, W. and W. R. Green. Murine AIDS requires CD154/CD40L expression by the CD4 T cells that mediate retrovirus-induced disease: Is CD4 T cell receptor ligation needed? *Virology* 360: 58-71.

Liang, B., J. Y. Wang, and R. R. Watson. 1996. Murine AIDS, a key to understanding retrovirus-induced immunodeficiency. *Viral Immunology* 9: 225-239.

Ma, C. 2010. The 4 Parameter Logistic (4PL) nonlinear regression model. MiraiBio Group Blog. < http://www.miraibio.com/blog/2010/08/the-4-parameter-logistic-4pl-nonlinear-regression-model/>. Accessed April 10 2013

Macagno, A., M. Gilliet, F. Sallusto, A. Lanzavecchia, F. O. Nestle, and M. Groettrup. 1999. Dendritic cells up-regulate immunoproteasomes and the proteasome regulator PA28 during maturation. *European Journal of Immunology* 29: 4037.

MacDonald, T. T. and J. Spencer. 1994. Lymphoid cells and tissues of the gastrointestinal tract. In *Gastrointestinal and Hepatic Immunology,* R. V. Heatley ed. Cambridge University Press, Cambridge. 1-23.

Makino, M., W. F. Davidson, T. N. Fredrickson, J. W. Hartley, and H. C. Morse 3. 1991. Effects of non-MHC loci on resistance to retrovirus-induced immunodeficiency in mice. *Immunogenetics* 33: 345-351.

Makino, M., H. C. Morse 3, T. N. Fredrickson, and J. W. Hartley. 1990. H-2-associated and background genes influence the development of a murine retrovirus-induced immunodeficiency syndrome. *The Journal of Immunology* 144: 4347-4355.

Malim, M. H. and M. Emerman. Review: HIV-1 Accessory Proteins—Ensuring Viral Survival in a Hostile Environment. *Cell Host & Microbe* 3: 388-398.

Mankan, A. K. and V. Hornung. 2012. Retroviral Danger from Within: TLR7 Is in Control. *Immunity* 37: 763-766.

Masur, H., J. E. Kaplan, and K. K. Holmes. 2002. Guidelines for preventing opportunistic infections among HIV-infected persons--2002. Recommendations of the U.S. Public Health Service and the Infectious Diseases Society of America. *Annals of Internal Medicine* 137: 435-478.

Maupin-Furlow, J. A., M. A. Gil, M. A. Humbard, P. A. Kirkland, W. Li, C. J. Reuter, and A. J. Wright. 2005. Archaeal proteasomes and other regulatory proteases. *Current Opinion in Microbiology* 8: 720-728.

Mishto, M., E. Bellavista, A. Santoro, A. Stolzing, C. Ligorio, B. Nacmias, L. Spazzafumo, M. Chiappelli, F. Licastro, S. Sorbi, A. Pession, T. Ohm, T. Grune, and C. Franceschi. 2006. Immunoproteasome and LMP2 polymorphism in aged and Alzheimer's disease brains. *Neurobiology of Aging* 27: 54-66.

Mosier, D. E. 1996. Small animal models for acquired immune deficiency syndrome (AIDS) research. *Laboratory Animal Science* 46: 257-265.

National Institute for Allergy and Infectious Diseases (NIAID). 2010. HIV Replication Cycle. <http://www.niaid.nih.gov/topics/HIVAIDS/Understanding/Biology/Pages/hivReplicationCycle.aspx>. Accessed 13 March 2013.

Noda, C., N. Tanahashi, N. Shimbara, K. B. Hendil, and K. Tanaka. 2000. Tissue distribution of constitutive proteasomes, immunoproteasomes, and PA28 in rats. *Biochemical and Biophysical Research Communications* 277: 348-354.

Okamoto, H. 1999. The Reg gene family and Reg proteins: with special attention to the regeneration of pancreatic β-cells. *Journal of Hepato-Biliary-Pancreatic Surgery* 6: 254.

Okulicz, J. F., V. C. Marconi, M. L. Landrum, S. Wegner, A. Weintrob, A. Ganesan, B. Hale, N. Crum-Cianflone, J. Delmar, V. Barthel, G. Quinnan, B. K. Agan, and M. J. Dolan. 2009. Clinical Outcomes of Elite Controllers, Viremic Controllers, and Long-Term Nonprogressors in the US Department of Defense HIV Natural History Study. *Journal of Infectious Diseases* 200: 1714-1723.

Palmowski, M. J., U. Gileadi, M. Salio, A. Gallimore, M. Millrain, E. James, C. Addey, D. Scott, J. Dyson, E. Simpson, and V. Cerundolo. 2006. Role of immunoproteasomes in cross-presentation. *The Journal of Immunology* 177: 983-990.

Parham, P. and C. Janeway. 2009. The immune system / Peter Parham. London, New York: Garland Science; 3rd ed.

Perry, M. J. 1998. Gender, race and economic perspectives on the social epidemiology of HIV infection: Implications for prevention. *The Journal of Primary Prevention* 19: 97-104.

Planas, R., I. Pujol-Autonell, E. Ruiz, M. Montraveta, E. Cabre, A. Lucas-Martin, R. Pujol-Borrell, E. Martinez-Caceres, and M. Vives-Pi. 2011. Regenerating gene Iα is a biomarker for diagnosis and monitoring of celiac disease: a preliminary

study. *Translational Research: The Journal of Laboratory & Clinical Medicine* 158: 140.

Reen, D. J. 1994. Enzyme-linked immunosorbent assay (ELISA). *Basic Protein and Peptide Protocols,* Springer, 461-466.

Rock, K. L., A. Y. Ian, T. Saric, and L. G. Alfred. 2002. Protein degradation and the generation of MHC class I-presented peptides. *Advances in Immunology* 80: 1-70.

Roses, S. 2013. Personal Communication.

Sáez-Cirión, A., G. Pancino, M. Sinet, A. Venet, and O. Lambotte. 2007. HIV controllers: how do they tame the virus? *Trends in Immunology* 28: 532-540.

Safavi, F. and A. Rostami. 2012. Role of serine proteases in inflammation: Bowman-Birk protease inhibitor (BBI) as a potential therapy for autoimmune diseases. *Experimental and Molecular Pathology* 93: 428-433.

Sherman, M. Y. and A. L. Goldberg. Review: Cellular Defenses against Unfolded Proteins. A Cell Biologist Thinks about Neurodegenerative Diseases. *Neuron* 29: 15-32.

Sparger, E. E., P. A. Luciw, J. H. Elder, J. K. Yamamoto, L. J. Lowenstine, and N. C. Pedersen. 1989. Feline Immunodeficiency Virus is a Lentivirus Associated with an Aids-Like Disease in Cats. *AIDS* 3: S43-S49.

Tanaka, K. and M. Kasahara. 1998. The MHC class I ligand-generating system: roles of immunoproteasomes and the interferon-gamma-inducible proteasome activator PA28. *Immunological Reviews* 163: 161-176.

Tepsuporn, S., J. N. Horwitt, G. W. Cobb, and S. A. Stranford. 2008. MAIDS resistance-associated gene expression patterns in secondary lymphoid organs. *Immunogenetics* 60: 485-494.

Terazono, K., H. Yamamoto, S. Takasawa, K. Shiga, Y. Yonemura, Y. Tochino, and H. Okamoto. 1988. A novel gene activated in regenerating islets. *Journal of Biological Chemistry* 263: 2111-2114.

UNAIDS. 2009. Global Report Fact Sheet: The Global AIDS Epidemic

UNAIDS. 2011. Global HIV/AIDS Response: Epidemic Update and Health Sector Progress Towards Universal Access.

UNAIDS. 2013. AIDSinfo Country fact sheets. Available at: http://www.unaids.org/en/dataanalysis/tools/aidsinfo/countryfactsheets/ (accessed March, 2013)

Unno, M., K. Nata, N. Noguchi, Y. Narushima, T. Akiyama, T. Ikeda, K. Nakagawa, S. Takasawa, and H. Okamoto. 2002. Production and Characterization of Reg Knockout Mice: Reduced Proliferation of Pancreatic β-Cells in Reg Knockout Mice. *Diabetes* 51: S478-S483.

Van Ba, I. A., S. Marchal, F. François, M. Silhol, C. Lleres, B. Michel, Y. Benyamin, J. Verdier, F. Trousse, and A. Marcilhac. 2012. Regenerating Islet-derived 1α (Reg-1α) Protein Is New Neuronal Secreted Factor That Stimulates Neurite Outgrowth via Exostosin Tumor-like 3 (EXTL3) Receptor. *Journal of Biological Chemistry* 287: 4726-4739.

van den Elsen, ,P.J., S. J. Gobin, van Eggermond M.C., and A. Peijnenburg. 1998. Regulation of MHC class I and II gene transcription: differences and similarities. *Immunogenetics* 48: 208-221.

Van den Eynde, B.J. and S. Morel. 2001. Differential processing of class-I-restricted epitopes by the standard proteasome and the immunoproteasome. *Current Opinion in Immunology* 13: 147-153.

Van Kaer, L., P. Ashton-Rickardt, M. Eichelberger, M. Gaczynska, K. Nagashima, K. L. Rock, A. L. Goldberg, P. C. Doherty, and S. Tonegawa. 1994. Altered peptidase and viral-specific T cell response in LMP2 mutant mice. *Immunity* 1: 533-541.

Van Kaer, L., P. Ashton-Rickardt, H. L. Ploegh, and S. Tonegawa. 1992. TAP1 mutant mice are deficient in antigen presentation, surface class I molecules, and CD4-8+ T cells. *Cell* 71: 1205-1214.

Viret, C., S. Leung-Theung-Long, L. Serre, C. Lamare, D. A. A. Vignali, B. Malissen, A. Carrier, and S. Guerder. 2011. Thymus-specific serine protease controls autoreactive CD4 T cell development and autoimmune diabetes in mice. *Journal of Clinical Investigation* 121: 1810-1821.

Weiss, R. A. 1993. How Does HIV Cause AIDS? *Science* 1273.

Whitelaw, E. and D. I. K. Martin. 2001. Retrotransposons as epigenetic mediators of phenotypic variation in mammals. *Nature Genetics* 27: 361.

Xu, Y. Y., K. Bhavani, J. R. Wands, and de la Monte S.M. 1995. Insulin-induced differentiation and modulation of neuronal thread protein expression in primitive neuroectodermal tumor cells is linked to phosphorylation of insulin receptor substrate-1. *Journal of Molecular Neuroscience* 6: 91-108.

Zhang, Y. W., L. S. Ding, and M. D. Lai. 2003. Reg gene family and human diseases. *World Journal of Gastroenterology* 9: 2635-2641.